GEOLOGY

Cenozoic evolution of the steppe-desert biome in Central Asia

N. Barbolini[1,2*†], A. Woutersen[1*†], G. Dupont-Nivet[3,4,5†], D. Silvestro[6], D. Tardif[7], P. M. C. Coster[8], N. Meijer[3], C. Chang[9], H.-X. Zhang[9], A. Licht[10], C. Rydin[2,11], A. Koutsodendris[12], F. Han[13], A. Rohrmann[3], X.-J. Liu[14], Y. Zhang[15], Y. Donnadieu[16,17], F. Fluteau[7], J.-B. Ladant[18], G. Le Hir[7], C. Hoorn[1*†]

The origins and development of the arid and highly seasonal steppe-desert biome in Central Asia, the largest of its kind in the world, remain largely unconstrained by existing records. It is unclear how Cenozoic climatic, geological, and biological forces, acting at diverse spatial and temporal scales, shaped Central Asian ecosystems through time. Our synthesis shows that the Central Asian steppe-desert has existed since at least Eocene times but experienced no less than two regime shifts, one at the Eocene–Oligocene Transition and one in the mid-Miocene. These shifts separated three successive "stable states," each characterized by unique floral and faunal structures. Past responses to disturbance in the Asian steppe-desert imply that modern ecosystems are unlikely to recover their present structures and diversity if forced into a new regime. This is of concern for Asian steppes today, which are being modified for human use and lost to desertification at unprecedented rates.

INTRODUCTION

The modern Palaearctic steppe is the largest ecoregion of its kind in the world, covering over 10 million km^2 across the midlatitudes of Eurasia (*1*). Its massive size and geographic position are instrumental in granting the steppe biome great climatic and ecological relevance, with the steppe-deserts across the Central Asian continental interior having particularly high levels of biodiversity (*1*–*3*). This region comprises Mongolia, northern and western China, and western and central (geographic) Tibet (Fig. 1), which all host typical steppes and are characterized by summer-dominated low precipitation and extreme seasonality (*1*, *2*). Together, they form the unique "Central Asian steppe-desert biome," which is today dominated by C_3/C_4 xerophilous grasses and herbs belonging to the Poaceae, Chenopodioideae [former goosefoot family Chenopodiaceae (*4*)] and Asteraceae (*5*–*7*). This vegetation supports a diverse mammal fauna with a number of regional endemics, including herbivorous burrowing rodents and lagomorphs, migrating wild ungulates, and carnivorous felids, canids, mustelids, and ursids (*1*, *8*, *9*). Steppes west of the Tian Shan/Altai mountains are more climatically and florally similar to European and Mediterranean grasslands and are instead termed "Middle Asia" (*1*, *2*). For a full description of how the steppe subregions are delineated, see Materials and Methods.

A markedly different steppe-desert existed in Paleogene times. Ancient Central Asian floras likely already exhibited high biodiversity and spatial variation (*10*), but overall, they were characterized by a predominance of shrubs, forest, and ferns rather than herbs (*5*, *11*–*14*). Today, these plant groups form fairly minor components of the steppe-desert flora across this region (*1*, *7*, *15*), but how, when, and why this change occurred remain to be revealed. Unfortunately, current Cenozoic records are insufficient for a detailed understanding of the origins and evolutionary history of the steppe-desert's unique modern biotas.

Several driving mechanisms may have contributed to forming present-day Central Asian biotic structures and distributions. It is thought that in response to the India-Asia collision, Tibetan topographic growth and the Eocene retreat of the inland proto-Paratethys Sea (Fig. 2) reduced moisture supply to Central Asia along with the late Oligocene to Miocene uplift of the Pamir and Tian Shan ranges, isolating the Taklimakan sand sea as well as the Tengger and other deserts further eastward [e.g., (*16*–*23*)]. Resulting long-term Cenozoic drying of the region may also relate to global cooling, reducing monsoons and the hydrological cycle (*16*, *24*, *25*), or the tectonically driven northward motion of the Tibetan region and associated atmospheric circulation systems (*26*–*28*). Disentangling the effects of these diverse climatic and geological forces on ecosystem evolution in Central Asia has proven challenging; extended palaeofloral reference sections with reliable age control are rare, hampering interbasinal and global correlation to environmental and climatic archives.

Of particular interest to understand Central Asian ecosystems are major synchronous transitions in vegetation and climate. Such a

[1]Department of Ecosystem and Landscape Dynamics, Institute for Biodiversity and Ecosystem Dynamics, University of Amsterdam, 1098 XH Amsterdam, Netherlands. [2]Department of Ecology, Environment and Plant Sciences and Bolin Centre for Climate Research, Stockholm University, SE-106 91 Stockholm, Sweden. [3]Universität Potsdam, Institute of Geosciences, 14476 Potsdam, Germany. [4]Université de Rennes, CNRS, Géosciences Rennes–UMR 6118, F-35000 Rennes, France. [5]Key Laboratory of Orogenic Belts and Crustal Evolution, Peking University, Beijing 100871, China. [6]Department of Biology, University of Fribourg, Ch. De Musée 10, Fribourg, Switzerland. [7]Institut de Physique du Globe, Paris 75005, France. [8]Biodiversity Institute, University of Kansas, Lawrence, KS 66045, USA. [9]Key Laboratory of Biogeography and Bioresource in Arid Land, Xinjiang Institute of Ecology and Geography, Chinese Academy of Sciences, Urumqi 830011, China. [10]Department of Earth and Space Sciences, University of Washington, Seattle, WA 98195, USA. [11]The Bergius Foundation, The Royal Swedish Academy of Sciences, Box 50005, SE-104 05 Stockholm, Sweden. [12]Institute of Earth Sciences, Heidelberg University, Heidelberg 69120, Germany. [13]School of Earth Sciences, East China University of Technology, Nanchang 330013, Jiangxi, China. [14]College of Geography and Environmental Science, Northwest Normal University, Lanzhou 730070, China. [15]The First Monitoring and Application Center, China Earthquake Administration, Tianjin 300180, China. [16]Laboratoire des Sciences du Climat et de l'Environnement (LSCE)/Institute Pierre Simon Laplace (IPSL), Commissariat á l'Énergie Atomique et aux Énergies Alternatives (CEA)-CNRS–Université de Versailles Saint Quentin-en-Yvelines (UVSQ), Université Paris-Saclay, Gif-sur-Yvette, France. [17]Aix-Marseille Université, CNRS, Institut pour la Recherche et le Développement (IRD), Collège de France, Centre de Recherche et d'Enseignement de Géosciences de l'Environnement (CEREGE), Aix-en-Provence, France. [18]Department of Earth and Environmental Sciences, University of Michigan, Ann Arbor, MI 48109, USA. *Corresponding author. Email: natasha.barbolini@su.se, barbolini.natasha@gmail.com (N.B.); amberwoutersen@gmail.com (A.W.); m.c.hoorn@uva.nl (C.H.) †These authors contributed equally to this work.

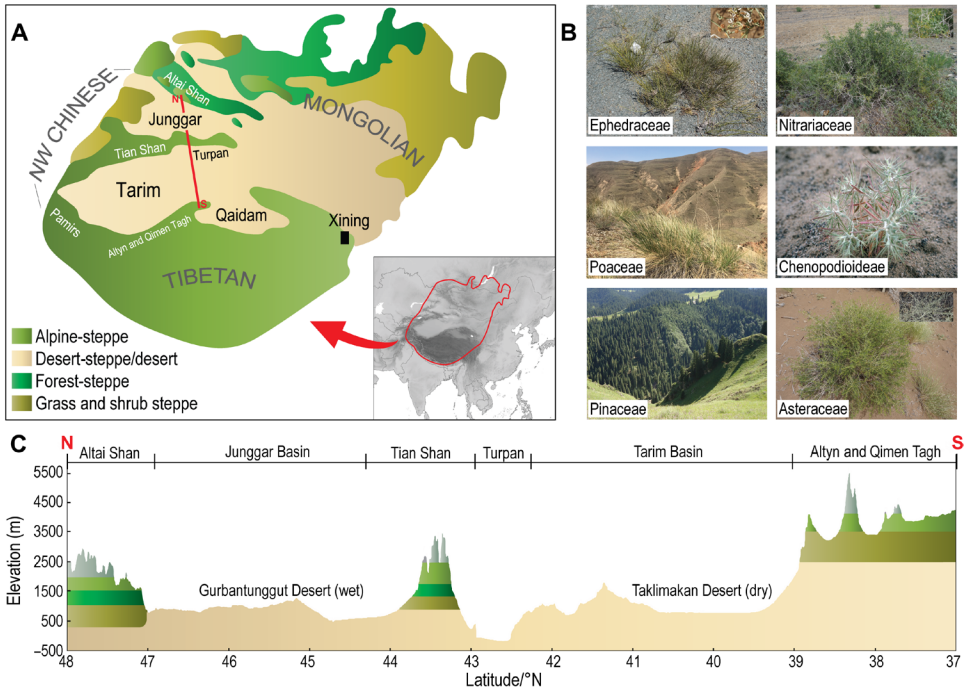

Fig. 1. The modern Central Asian steppe-desert. (**A**) Ecological-physiognomic steppe subtypes across the Tibetan, northwestern (NW) Chinese, and Mongolian regions, with sedimentary basins and mountain ranges marked in black and white, respectively [after (*1*, *11*, *97*)]. Location of the altitudinal profile in (**C**) is marked in red. (**B**) Characteristic plant families, represented by (clockwise from top left): *Ephedra* sp. (Ephedraceae), *Nitraria* sp. (Nitrariaceae), *Ceratocarpus* sp. (Chenopodioideae), and *Artemisia* sp. (Asteraceae): all common in desert steppe and desert; *Picea* sp. (Pinaceae: common in forest steppe); and *Achnatherum* sp. (Poaceae: common in grass and shrub steppe). The latter image was photographed in the Xining Basin, Qinghai Province (photo credit: Natasha Barbolini, University of Amsterdam); all other images were taken on the southern margin of the Junggar Basin/northern slope of the Tian Shan, Xinjiang Uyghur Autonomous Region (photo credits: Hong-Xiang Zhang, Xinjiang Institute of Ecology and Geography, Chinese Academy of Sciences). (**C**) Altitudinal profile illustrating vegetation belts of steppe subtypes shown in (A), with tundra and periglacial in gray.

transition, leading to the modern steppe biome, has been traditionally hypothesized to have occurred around the 23-Ma Paleogene–Neogene boundary (*11*, *29*–*33*), although it may well have taken place considerably earlier (*10*, *34*, *35*). Its nature and timing have remained largely unexplored because of a lack of well-dated, integrated palaeobotanical datasets. Recently, it has been recognized that the global climate event at the Eocene–Oligocene Transition (EOT) had a major and sudden regional environmental impact associated with aridification, a decrease in temperature, mammal turnover, and pronounced vegetation changes (*5*, *16*, *36*–*39*). This suggests significant ecosystem restructuring linked to a rapid EOT climate shift, but it remains unknown when and how biota recovered and if this may be linked to the later emergence of the modern steppe-desert.

Here, we present a high-resolution Cenozoic palaeovegetation reconstruction from the Eocene to Pleistocene. We first focus on original and recently published data from the Eocene greenhouse period and over the EOT global cooling, to establish the importance and nature of this transition. We then assess the long-term response to this change by reviewing vegetation, mammalian, and climatic records through the Oligocene and Neogene. This permits us to assess major driving factors of Central Asian steppe-desert ecosystem development until its modern establishment. We use a well-dated, temporally extensive "best record" (see Materials and Methods) from northeastern (NE) Tibet, integrated within a Central Asian compilation of previous palynological and palaeobiological studies, and original climate proxy data and model simulations, to identify key questions of ecosystem evolution in the Palaearctic steppe biome: When did the plant compositional transformation from a shrub- to herb-dominated biome occur in the Central Asian steppe-desert, and how have diverse climatic and geological forces shaped Asian ecosystems through the Cenozoic?

FROM EOCENE SHRUB DOMINANCE TO OLIGOCENE COLLAPSE (PHASE 1)

The Eocene steppe-desert

In the middle Eocene, the steppe-desert in what is today NE Tibet (eastern Central Asia) hosted a unique shrub vegetation that included halophytic (salt-tolerant) Nitrariaceae and xerophytic (drought-tolerant) Ephedraceae (Fig. 3). Xerophytic herbs such as Asteraceae, Chenopodioideae, and Poaceae formed very minor components of this steppe-desert ecosystem (Fig. 3), with broad-leaved forest (mainly temperate) and other angiosperms comprising most of the remaining pollen sum. Arboreal pollen sourced from higher elevations suggests repeated warm and humid conditions in the uplands during the middle Eocene (*5*). Herbaceous grasses (*Graminidites* pollen; Poaceae) can be traced back to the early Eocene (47.7 Ma; Fig. 3) but remain minor compared to the prevalence of the shrub group at this time. This extends the age-constrained record of grass pollen in Central Asia to ca. 25 Ma before early Miocene records from northwestern China (*40*–*42*) previously considered to be the oldest appearances.

At ca. 40 Ma, Nitrariaceae and Ephedraceae became increasingly predominant over angiosperm tree and herbaceous taxa, and by the late Eocene, ca. 37 Ma, conifer taxa that occupy higher altitudes today [*Picea* and *Abies*; (*5*)] began to appear. This suggests a shift to a cooler,

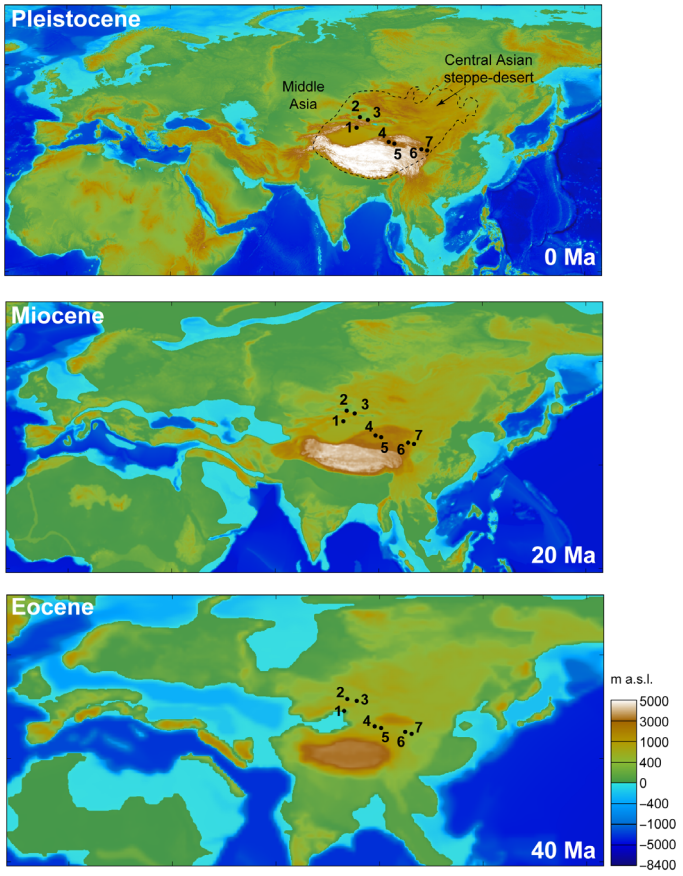

Fig. 2. Geographic setting of Central Asian pollen records reviewed here. Reconstructed palaeogeographies at 40 Ma (middle-late Eocene), 20 Ma (early Miocene), and 0 Ma (Pleistocene/modern) show progressive Tibetan orogenic growth and westward retreat of the proto-Paratethys Sea from the Eocene until the modern day. Colors indicate meters above sea level (m a.s.l.); a low (≤2 km) to moderate (~3 km) elevation characterized Central Asia in the Eocene [(*152*, *162*); https://map.paleoenvironment.eu/], while a high elevation (~4.5 km) exists in the Tibetan region today. 1, southern Tian Shan; 2 and 3, northern Tian Shan; 4 and 5, Qaidam Basin; 6, Xining Basin; 7, Lanzhou Basin. For details of how palaeogeographic reconstructions were derived, see Materials and Methods; for individual pollen records, see fig. S1.

drier environment in the uplands of eastern Central Asia (Fig. 3). These two steps are respectively coeval with subsequent retreats of the proto-Paratethys Sea that promoted the aridification of the Asian interior (*43*). The 37-Ma conifer appearance is also linked with a pronounced cooling event (although not as great as the later EOT temperature shift; Fig. 3) followed by a period of late Eocene climatic instability (*39*). Despite these temperature fluctuations, vegetational structure remained relatively consistent until global cooling at the EOT.

Evidence for biotic collapse at the EOT

The EOT is described as a two-stepped isotopic event in marine records comprising EOT-1 ca. 34.0 Ma, interpreted as mainly cooling, and Oi-1 ca. 33.5 Ma, interpreted as mainly glaciation (*44*, *45*) and reflected in eastern Central Asia by a large drop in carbonate growth temperatures due to both cooling and a reduction in summer precipitation (Fig. 3) (*39*). Both events can be distinguished in the pollen record: EOT-1 was synchronous with a rapid, large crash in abundance and diversity of the dominant Nitrariaceae-Ephedraceae shrubs (from two-thirds to half of the pollen sum), while conifer pollen (Pinaceae) increased markedly in both abundance and diversity (Fig. 3). Temperate broad-leaved forest pollen also increased slightly but, unlike the conifers, showed no increase in diversity (*39*). The above vegetation trends continue through Oi-1 and into the early Oligocene, when the formerly dominant shrubs virtually disappeared from the landscape. The xerophytic herbs, which dominate cold-temperate environments in Central Asia today (*6*, *7*), did not increase at all over the EOT nor in the early Oligocene (Fig. 3) despite the shrub disappearance as well as a precipitation drop suggested by clumped isotopes (*39*) and climate model simulations (*46*).

In other rare Oligocene palynological sites from Central Asia, xerophytic herbs also remained at comparatively low proportions of the Oligocene vegetation, despite sedimentological evidence indicating a shift to a drier climate (*13*, *38*, *47*). Further to the south, the shrub disappearance remains undocumented: Latest Paleocene to late Oligocene fossil biota from central Tibet (southern Central Asia) instead indicate substantial topographic variation that hosted tropical/subtropical forests in valleys to mixed coniferous-broadleaved forest in highlands (*48*–*52*). This region is now alpine steppe (Fig. 1), revealing that central Tibet only became part of the interior Asian steppe-desert biome sometime in the Miocene. The EOT and Oligocene thus remain poorly documented periods for the Central Asian steppe, but to date, known vegetation shifts in the interior of Central Asia are consistent with previous studies from late Eocene and early Oligocene sections documenting conifer taxa in the peripheral mountains, broad-leaved deciduous woodland on slopes and in river valleys, and xerophytic shrubs dominating lower-altitude valley basins (*5*, *12*, *14*, *17*, *38*). This illustrates the complexity of the topographic relief in eastern Central Asia at this time, supporting the view that an extensive high plateau only formed in this region later (*52*).

The pollen record in eastern Central Asia thus incorporates a multitude of plant taxa that coexisted in different parts of the environment; accordingly, there was probably no direct competition and replacement of the dominant shrub group by conifers over the EOT. Rather, the large increase of arboreal pollen in the record likely reflects a decrease of vegetation cover at lower altitudes, which is supported by various lines of evidence from other proxies.

First, climate model simulations (see Materials and Methods) for eastern Central Asia over the EOT predict a doubling of bare soil proportion [20 to 50%, Fig. 4C (III)] in the NE Tibet area and a marked increase of conifers in the surrounding northern regions (up to 40 to 60% increase in the Turgai area) as well as over the Tibetan region [Fig. 4C (IV)]. These climatic changes over the EOT are associated with cooling of ~9°C [Fig. 4C (I)] along with a drop of cold month mean temperature (CMMT) below freezing (table S2) and a decrease in mean annual precipitation (MAP) by −25 to −50% [from ~500 to ~250 mm/year; Fig. 4, A (II) to C (II)]. Conifers (gymnosperms) can outcompete deciduous angiosperm trees under these conditions (*53*, *54*), which could explain the rapid diversification of Pinaceae in the eastern Central Asian pollen record. The role of the atmospheric carbon dioxide concentration (pCO_2) drop over the EOT (*55*, *56*) appears less important than temperature. Tropical conifers are more responsive to atmospheric pCO_2 than tropical angiosperms, showing improved growth and water use efficiency under higher CO_2 (*57*). Despite this, conifers have demonstrated range expansions during cooler periods with lower atmospheric pCO_2 (*57*), as is observed in Central Asia (Fig. 3). In addition to the large expansion of conifers (Fig. 3) and climate simulations for the region suggesting

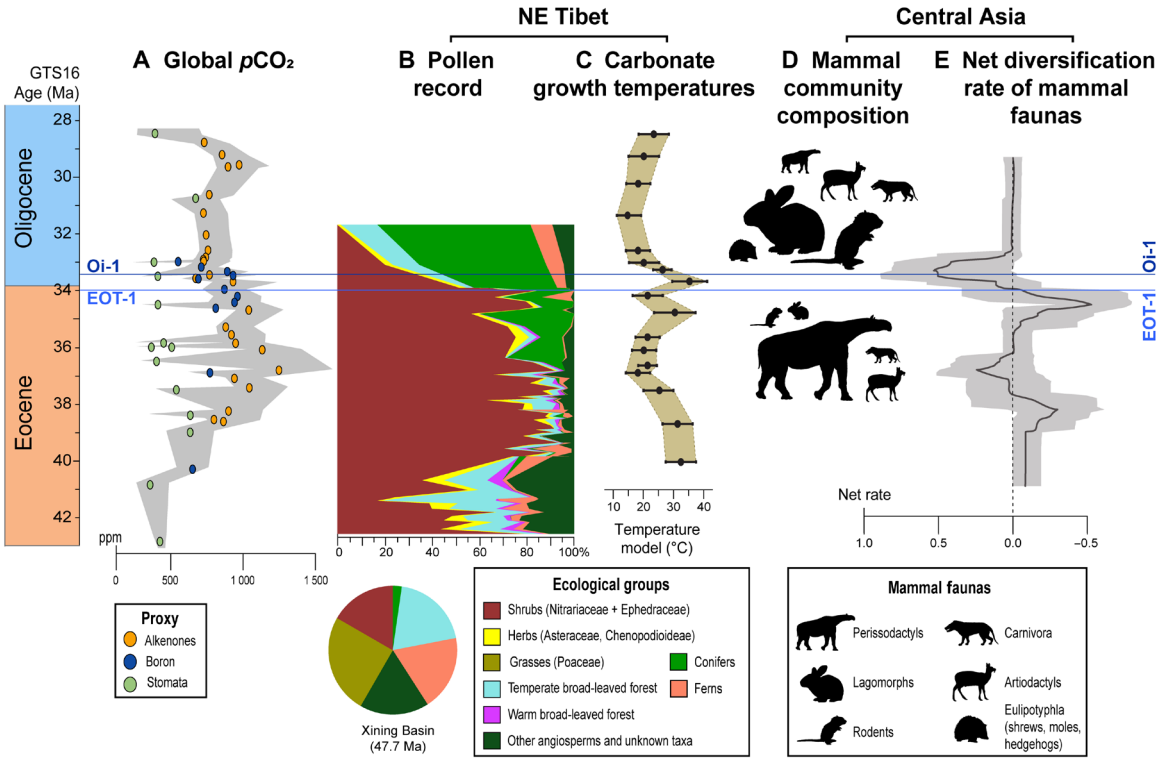

Fig. 3. High-resolution changes over the EOT in Central Asia. Global atmospheric carbon dioxide concentration (pCO_2) variation over this period is derived from various proxies (**A**) (*163*, *164*); ppm, parts per million; GTS16, Geologic Time Scale: 2016 (*165*). Vegetation (**B**) (this study; table S6) and temperature (**C**) [Page *et al.* (*39*)] from an extended Eocene–Oligocene reference section in NE Tibet are plotted against faunal changes in Central Asia [see Materials and Methods for details of how (D) and (E) were compiled]. Silhouette sizes indicate the proportional abundance of clades in Eocene and Oligocene mammalian communities. Net diversification rates show a strong drop in diversity (negative net rate) at the Eocene–Oligocene Boundary, followed by a rebound with strongly positive diversification rate in the early Oligocene.

CMMT below freezing (Fig. 4), Climate Leaf Analysis Multivariate Program (CLAMP) analysis on fossil leaves from the Qaidam Basin also indicates near-freezing (1.4° ± 3.5°C) winters in the early Oligocene (*12*).

Second, analyses of the fossil record of Central Asian mammal biota (Fig. 3) illustrate the pronounced faunal turnover and notable decrease in body size across the EOT known from studies in Mongolia and northwestern China (*36*–*38*, *58*). This turnover, from perissodactyl-dominant Eocene faunas to rodent/lagomorph-dominant Oligocene faunas, suggests an environment that could support significantly reduced vegetation biomass after the EOT and would thus have favored smaller mammals.

Third, modern studies of sparsely vegetated, cold, and arid areas from sites at a wide elevational range across Eurasia (*7*, *59*–*62*) demonstrate that pollen records from these areas contain an inflated component of wind-transported arboreal pollen, similar to what is observed in NE Tibet over the EOT. Accordingly, all data (Figs. 3 and 4) point toward a shift to a more open, seasonally arid environment, with an altered precipitation regime and winter freezing in eastern Central Asia over the EOT.

A REGIME SHIFT AT THE GREENHOUSE TO ICEHOUSE TRANSITION

"Catastrophic regime shifts" are documented from a range of ecosystems: They involve a marked shift from one ecosystem state to another and can occur either because of a sudden large external impact or gradual smaller changes that continue until a critical threshold is reached (*63*). All evidence shows that the EOT is concurrent with a marked regime shift in the Central Asian steppe-desert, involving the most pronounced environmental changes in the Cenozoic. Was this regime shift the result of a single large event (i.e., a rapid decline in atmospheric temperature and pCO_2) or did it combine with more gradual changes in the Eocene [climatic fluctuations (*39*), aridification (*16*, *43*, *64*), and/or tectonic activity (*52*, *65*)] that eroded ecosystem resilience until the maximum threshold was reached at the EOT?

Role of the proto-Paratethys Sea retreat before the EOT

The extended Eocene record (Fig. 3) is ideally placed to answer this question. In the Central Asian continental interior, the EOT was preceded by long-term sea retreat of the proto-Paratethys Sea from Eurasia, which was driven primarily by tectonism [e.g., (*43*)] modulated by stepwise sea level drops as global temperatures declined leading to the growth of the Antarctic Ice Sheet (*16*, *19*). Over time, sea regression removed a major source of moisture from the Asian interior, and this drying trend particularly intensified stepwise in relation to sea regressions ca. 40 and 37 Ma (*19*, *43*, *64*, *66*), placing vegetation under increasingly limited moisture restrictions from the middle–late Eocene. Global cooling as well as continuing north- and southward outward growth of the northern and central Tibetan Highland in the Eocene (*26*, *28*, *65*, *67*) may also have contributed toward long-term aridification in the continental interior (*22*, *64*), but the pollen record shows that vegetation response to proto-Paratethys Sea regressions was more substantial: After the 40- and 37-Ma regressions, halophytic and xerophytic shrubs (Nitrariaceae and Ephedraceae)

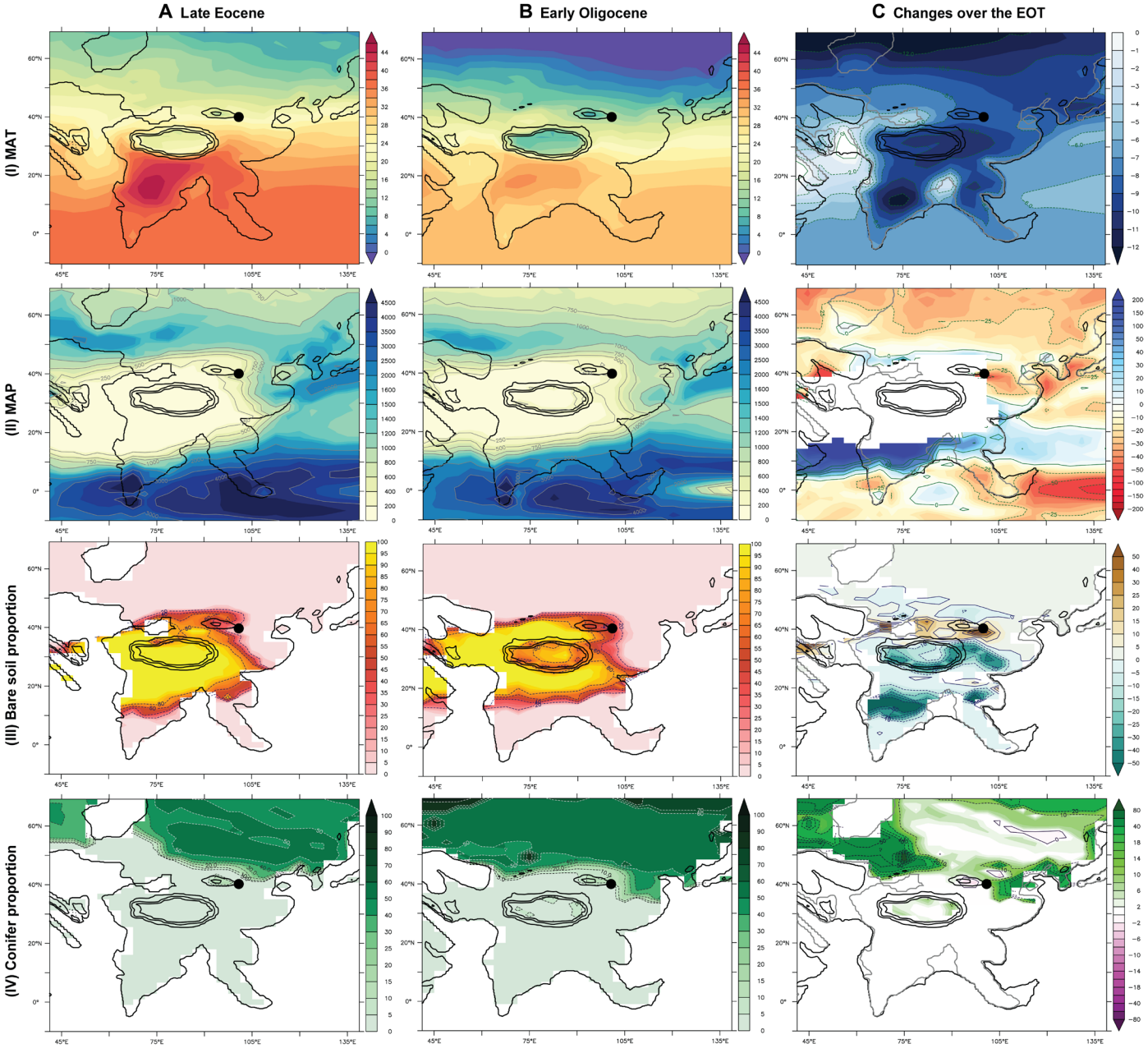

Fig. 4. Late Eocene and early Oligocene climate simulations for Central Asia. The Xining Basin in NE Tibet is indicated by a black circle. Simulations show (I) mean annual temperature (MAT), (II) mean annual precipitation (MAP), (III) bare soil proportion, and (IV) conifer proportion for (**A**) the late Eocene, (**B**) the early Oligocene, and (**C**) changes over the EOT [expressed as Oligocene minus Eocene in degrees Celsius (C-I) and percent (C-II, C-III, and C-IV)]. All anomalies are obtained through a Student's *t* test and are significant at 95% confidence. Topography is represented by thick contours (each 1000 m of elevation). Thin numbered contours refer to each plot shading. In (C-II), the white area represents persistent arid zones in simulations (<300 mm/year).

comprised a far greater proportion of the steppe vegetation, while broad-leaved tree and other angiosperm diversity was immediately much reduced (Fig. 3). This response is also observed in other Central Asian basins including Tarim and Qaidam, although dating is less well constrained (*12*, *68*, *69*). This "aridification pathway" in response to the drying of the Tarim Basin after the final proto-Paratethys Sea regression is also clear from our modeling results [Fig. 4C (III)] with the development of a band of increased bare soil fraction at 40°N along the westerlies pathway. Through sensitivity experiments (testing the effect of an atmospheric pCO_2 drop only versus a pCO_2 drop and sea level retreat), the aridification of this region can be attributed unequivocally to the sea level change (fig. S2).

Reaching the threshold for a permanent shift at the EOT

Before the EOT, we hypothesize that Nitrariaceae-Ephedraceae shrub vegetation endured late Eocene aridification and cooling in the

same way as modern arid systems. In water-limited environments today, existing vegetation is known to endure by modifying the abiotic environment in a self-beneficial manner that promotes further plant growth: This includes decreasing runoff and concentrating local moisture and nutrients in the topsoil, reducing albedo and soil evaporation, preventing erosion, and increasing regional rainfall (*70*, *71*). Alternative stable ecosystem states (i.e., vegetated or nonvegetated) can thus occur over a range of precipitation levels because of this feedback loop, and accordingly, once vegetation patches are lost, they cannot easily reappear (*72*). These "islands of fertility" are essential for dryland ecosystem structure and functioning, but once an aridity threshold is reached, saprotrophic fungi—key in maintaining vegetation patches—decrease rapidly (*73*, *74*). Aridity is a primary mechanism of steppe desertification in Central Asia today [e.g., (*75*, *76*)], particularly in highly precipitation-limited steppe-deserts where *Nitraria* and *Ephedra* exist under MAP of typically <100 mm (*11*). Beyond aridity values of 0.8 [calculated as 1 − (precipitation/potential evapotranspiration)], severe declines in plant cover and plant diversity, major species turnover, and exponential increases in albedo are observed in modern drylands (*73*). This is consistent with available evidence of major ecosystem changes at the EOT (Figs. 3 and 4).

At the EOT, our synthesis indicates a regime shift in Central Asia that was unidirectional in nature, meaning that once ecosystems had shifted into new and locally stable "equilibria," they did not return to their former biotic configurations. Pollen and mammal records (Fig. 3), as well as climate simulations (Fig. 4) all indicate that rapid cooling and increased seasonal aridity at the EOT caused a widespread loss of shrub biomass, thinning plant density, and likely a loss of plant diversity as well (although this remains to be demonstrated with molecular and pollen records). Lower-elevation landscapes would have become virtually barren, and only the vegetated peripheral mountain slopes provided palynological input. This represented a catastrophic shift to a new environmental state, previously recognized in the sedimentological record as a change from a "wet" desert with ephemeral saline lakes and mudflats within the basins, to a more arid desert with no lakes in many parts of Central Asia (*16*, *64*, *77*, *78*). A drop in atmospheric pCO_2 would have decreased water use efficiency, thus enhancing the effect of increased aridity (*57*). An atmospheric pCO_2 drop could also have played an important role in differential survival of Asian plant species over the EOT, which requires further investigation.

A general lack of vegetation cover would have stripped soils of their physical protection from wind, sun, and runoff, leading to extensive erosion, crust formation, and soil evaporation. Therefore, environmental conditions (temperature, precipitation, seasonality, atmospheric pCO_2, substrate, and soil biotas) fundamentally changed over the EOT, and despite temperature (*39*) and moisture (*13*, *79*) amelioration in the early Oligocene, water concentration in the topsoil could have been too low for seedlings to recolonize lower-altitude steppe-desert landscapes. Accordingly, vegetation would have been restricted to higher elevations with orographically derived moisture, consistent with pollen records comprising mainly arboreal pollen after the EOT (Fig. 3). Tectonic activity since the late Eocene created appropriate ecospace for conifers to expand at higher altitudes (*12*), but shifts coincident with Oi-1 glaciation are too sudden to be linked with tectonically driven altitudinal changes rather than cooling (*39*). In the high-resolution record for the EOT in the Xining Basin, sufficient age control enables the observed changes to be correlated with established climatic events in the marine realm and thus to be distinguished from tectonism (*16*). Widespread loss of vegetation cover at lower altitudes would have further decreased regional precipitation and increased albedo, perpetuating and possibly even amplifying cooling as observed in our temperature records at 37 Ma and the EOT (Fig. 3).

Impact on mammal biota

In turn, these large-scale palaeoenvironmental changes were likely responsible for the major, abrupt shift in Central Asian mammal biotas at the EOT termed the Mongolian Remodelling (*36*, *37*). This event was essentially synchronous with the European Grande Coupure in western Eurasia, and notably, both turnovers favored smaller rodent- and lagomorph-dominated communities at the expense of larger mammals (*37*, *38*, *80*, *81*). This has been attributed primarily to climate change creating more open, seasonal environments with lower resource availability across Eurasia, which would have exerted selective pressure on body size (*82*). Pronounced environmental changes in Central Asia support this argument, as does floral turnover from EOT reference sections in England (*80*), France (*83*), and Spain (*81*).

It is remarkable that the Mongolian Remodelling and Grande Coupure appear to have been synchronous and similar in nature, despite the very different floras in Central Asia and Europe both before and after the EOT. While Asian vegetation was already dominated by xerophytic, arid-adapted shrubs before the EOT (Fig. 3), Europe hosted predominantly more humid, paratropical/subtropical evergreen, and warm-temperate mixed forests in the late Eocene (*84*) [although many southwestern European floras from this period have xeromorphic leaves (*85*)]. Over the EOT, greater aridity and frost in Central Asia promoted the spread of cool-temperate conifers (Fig. 4), which are poorly digested by mammals, can contain toxic compounds, and generally comprise low foliar nutrition compared to angiosperm tree taxa (*86*). In contrast, subtropical evergreen and mixed forests remained common in Europe during the early Oligocene (*84*), representing better food resources for mammals. Rodents have been found to use conifers as a food source (particularly the seeds) more effectively than browsing ungulates (*87*, *88*), but it is unknown whether these dietary preferences would also have applied in the Oligocene. Furthermore, the Mongolian Remodelling probably did not involve direct competition between large and small mammals for food resources, while dynamics of the Grande Coupure may have been influenced through the arrival of Asian immigrants (*36*) who would have been preadapted to feeding on more xerophytic vegetation already in the Eocene. However, if this did occur, then timing of the events suggests that Asian taxa likely originated from pre- as opposed to post-Mongolian Remodelling faunas (*37*).

Although the dynamics of these faunal extinctions require further clarification, it is clear that in Central Asia, lophodonty (hard elongated molar ridges) and hypsodonty (high-crowned molars) were already developed in Oligocene primary consumers including ochotonid lagomorphs, ruminant artiodactyls, and rodents (*36*), the latter of which display dental microwear patterns comprising primarily fine scratches (*89*). These dentary patterns are linked to exploitation of silica-rich or lower-quality resources (e.g., fibrous, old, or woody plant material) and/or additional intake of extraneous grit or soil and were previously thought to correlate with the development of grasslands [see discussion in (*40*)]. However, faunal hypsodonty is now used as a proxy for open and dry habitats generally (*40*), and high hypsodonty in Asia thus reflects the increased abrasiveness of

vegetation that developed over the EOT, as well as possibly increased soil erosion, and feeding at or below ground level (*90*, *91*). Increased levels of hypsodonty are commonly linked to a lowering of primary productivity, such as is found in seasonally or permanently arid and/or cold climates (*82*). Therefore, high levels of hypsodonty throughout the Miocene in Central Asia (*90*) reinforce palynological evidence for a dry belt across Asian midlatitudes that persisted from the early to early late Miocene (*92*).

FROM OLIGOCENE DESERT (PHASE 2) TO MIOCENE HERB STEPPE (PHASE 3)

Oligocene and early Miocene lowland deserts

The pollen record shows that the shrubs Nitrariaceae and Ephedraceae comprised the major component of the steppe-desert flora before the EOT. Subsequently, these shrubs either were absent from regional records or remained at comparatively low levels (Fig. 5), suggesting that they never recovered their former position of ecological prominence in Central Asia. However, shrub demise at the EOT was not a result of direct competition or replacement by herbs, which only began to consistently form significant components of Central Asian ecosystems 20 Ma later (see below). These data, together with mammal records (Fig. 5) (*36*, *89*, *90*, *92*), provide further support for widespread Oligocene and early Miocene aridity in Central Asia through a trend toward less representation of local (basinal) taxa, as overall vegetation cover at lower altitudes remained minimal. Instead, records are dominated by downslope transport of arboreal pollen from the lower montane vegetation belt (during phase 2; Fig. 5).

This interpretation differs from previous studies not recognizing the dominance of the downslope component and thus inferring a humid climate and the onset of steppe in parts of Central Asia from forest-dominated pollen records with the appearance of herbaceous components around the Paleogene–Neogene boundary [e.g., (*11*, *29*, *30*, *33*, *93*–*95*)]. These changes are coeval with the onset or reactivation of tectonic uplift of the Pamir, Tian Shan, Qilian Shan, and other Tibetan ranges (*20*, *96*), which forced orographic rainout and amplified a vegetational gradient that had already become established in the late Eocene: semiarid woodlands on slopes and in river valleys, but little vegetation occupying arid intermontane basins.

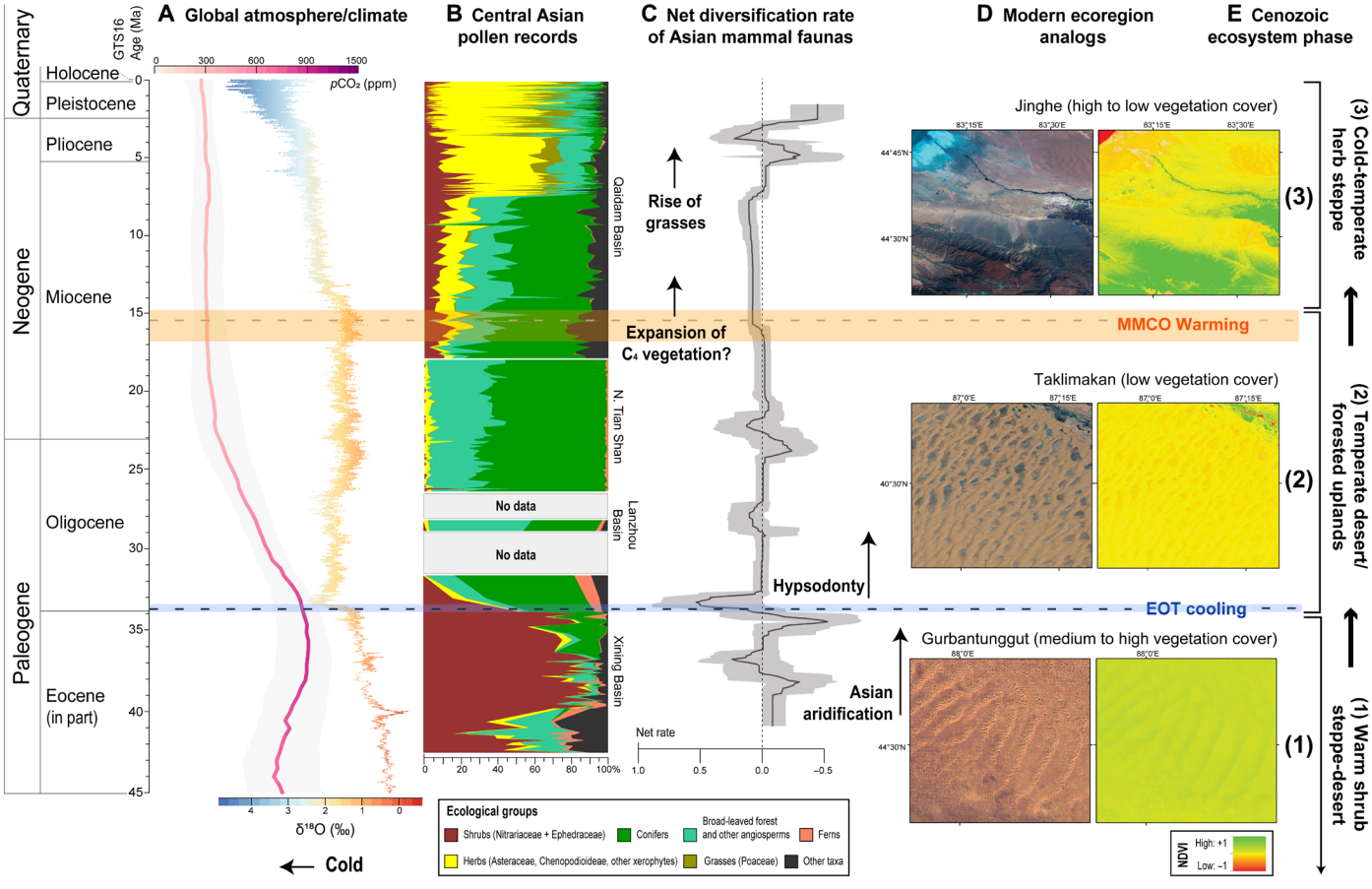

Fig. 5. The triphase Cenozoic history of the Central Asian steppe-desert biome. Vegetation changes are illustrated by a composite pollen record over the last ~43 Ma (**B**), within the context of global climate variation (**A**) and linked to net diversification rates of Central Asian mammalian communities (**C**). Extant Asian deserts are used as ecoregion analogs (**D**) for each ecosystem phase (**E**) and illustrated by natural view [left; images from Landsat 8 OLI (Operational Land Imager), https://glovis.usgs.gov/] and hyperspectral (right) normalized difference vegetation index (NDVI) models of the (1) Gurbantunggut Desert, (2) Taklimakan Desert, and (3) Jinghe mountain–desert ecotone. Atmospheric carbon dioxide concentration (pCO_2) is based on a LOESS (locally estimated scatterplot smoothing) fit through data from various proxy methods (*163*), enveloped by a 95% confidence interval in light gray. Global climate is represented by a nine-point moving average through the benthic foraminifera $\delta^{18}O$ record of Cramer *et al.* (*166*). For individual pollen records, see fig. S1; for statistical support of the three ecosystem phases, see fig. S3.

However, early Miocene uplift of these ranges was not sufficient to cause the spread of prominent herb-dominated steppes that would only happen millions of years later, from the mid- to late Miocene onward, ca. 15 Ma (Figs. 5 and 6) (*97*–*103*). This suggests that following such extended dry conditions since the EOT, combined with a lack of positive feedback mechanisms from existing vegetation to promote new plant growth (as discussed in the previous sections), other drivers besides enhanced topography were necessary to enable the reestablishment of vegetation biomass (and spread of the herbs) across Central Asian landscapes. These global to local climatic, geological, and biological drivers of ecological changes, combined to set in motion the turnover from a shrub- to herb-dominated biome in Central Asia, which we explore in the next section.

Emergence of the modern herb-dominated steppe biome

In Central Asia, molecular phylogenies of the angiosperm flora indicate that the steppe-desert ecosystem has served as an evolutionary cradle for herbaceous genera since the early Oligocene (*32*). Yet, there is a far longer time lag between the diversification and dominance of herbs, including grasses, in Central Asia (Fig. 5) compared to habitats across Eurasia and North America (*40*, *102*, *104*). While Asian semiarid and open habitats have hosted grasses in Central Asia since at least the middle Eocene (Fig. 3), widespread grass expansions did not occur before the mid-Miocene (Fig. 6). This extends the delay between taxonomic and ecological radiation of the C_3 grasses in Central Asia to at least 30 Ma, compared to ca. 10 Ma in other parts of the Eurasian steppe biome (*40*).

In the Asian steppe-desert, grass presence first rises to prominence at ~15 Ma, followed by a further increase at ~7 Ma (Fig. 6), the latter coinciding with the global rise of the grasses (*40*, *105*, *106*). Notably, there is a larger and earlier spread of grasses in eastern Central Asia, while in western Central Asia, the grasses do not have a meaningful presence in the fossil record until ~7 Ma (Fig. 6). Such variation is not recognized in the abundances of Nitrariaceae and Ephedraceae, which in none of the basins reappear to the high levels of the late Eocene (*6*, *97*–*101*, *103*, *107*–*110*).

The remarkable geographic difference in the spread of grasses from east to west is most likely related to environmental moisture differences in these alpine and temperate steppe environments. In western Central Asia, the dominant xerophytic herbs from the late Miocene onward are Chenopodioideae and *Artemisia* (fig. S1), suggesting that arid steppe-deserts and deserts were prevalent across this region. In contrast, the higher presence of grasses in eastern Central Asia indicates alpine and temperate steppe environments, which are comparatively higher in environmental moisture. This is in accordance with the eastern sites mostly being situated at higher elevations than those in the west since the Miocene (Figs. 2 and 6). It is also consistent with a strong east–west moisture gradient observable today in Central Asia (*111*), reaching most of the eastern sites (except 4 and 5 in the Qaidam Basin, Fig. 6) but not the western sites. A moisture driver is also suggested by the early grass emergence in the east ca. 15 Ma, coeval with the mid-Miocene climatic optimum (MMCO) that notoriously enhanced Asian monsoons (*112*).

Note that grasses (Poaceae) can be used as a proxy for moisture in the Central Asian steppe-desert. In the modern and Holocene steppe-desert, Poaceae together with *Artemisia* (Asteraceae) generally dominate more humid habitats (alpine/temperate grass steppe), while Chenopodioideae together with Asteraceae prefer more arid habitats (temperate/alpine/gobi deserts and desert-steppes; Fig. 1) (*7*, *61*). Modern ecological preferences of these dominant steppe-desert taxa probably would have been similar in the Neogene because (i) Global temperatures were cooling by the late Miocene (~11.6 to 5.3 Ma) to approach modern levels (Fig. 5); (ii) atmospheric pCO_2 concentrations were likely only moderately higher compared to preindustrial values [between ~450 and 550 parts per million (ppm) even in the MMCO; (*113*)]; and (iii) by the early Miocene, moderate to high elevations were starting to develop across much of the Tibetan and NW Chinese regions (Fig. 2).

Impact on mammals

After the crisis at the EOT, mammal diversity records a singular event at the Paleogene–Neogene boundary but is largely unaffected by the

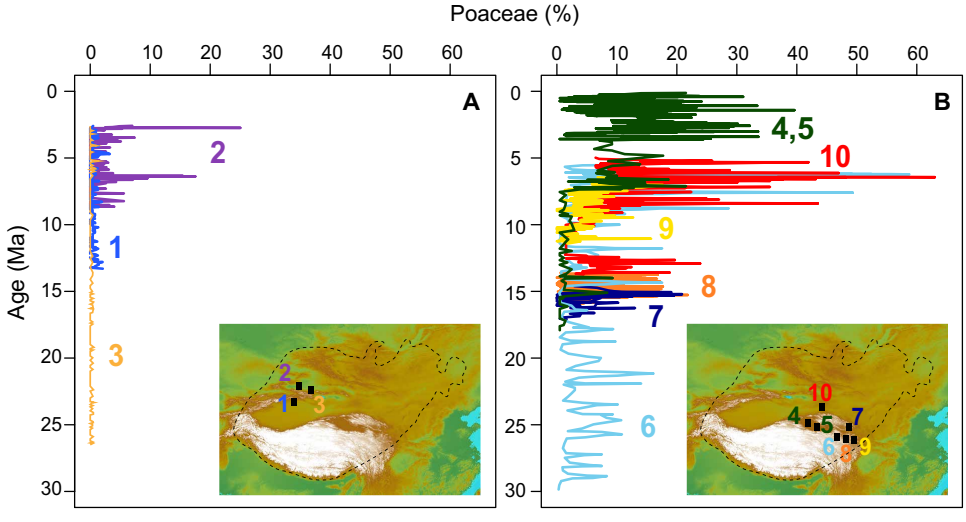

Fig. 6. The ecological rise of grasses across the Central Asian steppe-desert. This occurred gradually but was more restricted in the west (**A**) compared to the east (**B**). References for pollen data are as follows: (1) Zhang and Sun (*108*); (2) Sun *et al.* (*97*); (3) Sun and Zhang (*103*); (4 and 5) Miao *et al.* (*107*), Cai *et al.* (*109*), Koutsodendris *et al.* (*6*), and this study; (6) Li *et al.* (*110*); (7) Hui *et al.* (*99*); (8) Hui *et al.* (*98*); (9) Liu *et al.* (*100*); and (10) Ma *et al.* (*101*).

emergence of the herb-dominated steppe in the mid-Miocene ca. 15 Ma (Fig. 5). Although geographic coverage and chronology needs improvement, the interval between ca. 7 and 4 Ma is broadly concurrent with a high mammal turnover and associated immigration of regional faunas into northern China linked to a poorly defined "humid phase" (*97*, *114*, *115*). This is reflected in our data by two drops in net diversification: the first at 7 Ma indicating decline of the Miocene mammalian community, followed by a second, larger drop at 5 Ma and subsequent recovery in the late Pliocene ca. 4 Ma (Fig. 5). It is well documented that Plio–Pleistocene climatic fluctuations had considerable effects on shaping the present distributional ranges and genetic diversity of Asian floras and faunas [e.g., (*116*)], but by this time, dominance of the herb group was firmly established within Central Asia. Subsequent dynamics within plant communities were driven primarily by glaciation events, seasonal shifts in precipitation, and monsoonal variability (*6*, *97*, *103*, *107*, *109*), which all likely combined to give rise to mammalian extinctions in the Pleistocene (Fig. 5). Although the Neogene thus records several geographically diachronous faunal and floral changes, these did not all occur simultaneously as the result of a regime shift that can be constrained to a single point in time, such as at the EOT (Fig. 5).

DRIVERS OF NEOGENE RECOVERY TO MODERN STEPPE-DESERT

Mountain uplift

By the Miocene, regional tectonics and localized topography had created a highly varied landscape across the steppe-desert, with the Tibetan region (eastern Central Asia; Fig. 1) in particular serving as a center for plant diversification since at least the early Miocene [e.g., (*3*, *117*)]. Molecular phylogenetic analyses reveal that diversification in both the alpine biome [e.g., (*3*, *118*)] and steppe-desert lowlands (*119*–*121*) occurred during the mid- to late Miocene, which appear to be driven mainly by cooling and progressive aridity, respectively. This may be related to the generalized northward expansion of the Tibetan Highland and mountain ranges in the vicinity, including uplift of the Tian Shan, Pamir, Kunlun, and Qilian Shan-Nan Shan (*122*, *123*). This would have generated orographic rain shadows that appear to have modified precipitation patterns across relatively short distances during successive phases of orogeny (*18*). Although elevated parts already existed in remote northern and south-central Tibet in the late Eocene and Oligocene (*12*, *17*, *52*), further Miocene topographic growth of local ranges would also have increased the number of altitudinal climatic belts (ranging from alpine to lowlands), thus promoting local species richness and differing species compositions at regional scale [(*3*) and references therein].

Asian monsoons and westerly moisture

The expansion of herb-dominated steppes appears strongly correlated to increased moisture levels in Central Asia (Fig. 6), which is further substantiated by the characteristic moist steppe ecospace occupied by the Poaceae today (see the previous section). In Central Asia during the Neogene, moisture may be related to the combined effects of mountain building and climate changes expressed regionally as the Asian monsoons or westerlies (*124*, *125*). The initial expansion of herb steppes at ca. 15 Ma in the east (Fig. 6) coincided in time with the MMCO and linked intensification of the Southeast Asian monsoons (*10*, *126*). Although the Miocene records a strengthening of the Asian monsoons in response to general growth of the Himalaya-Tibetan orogen [e.g., (*127*)], a causal relationship is difficult to establish because of controversial estimates on the timing of monsoon intensification and plateau growth since at least the early Miocene [e.g., (*128*)].

Westerly moisture certainly affected herb steppe expansion, as it constitutes the dominant Central Asian moisture source of the western sites and probably also contributed to the eastern sites (Fig. 6). It is now generally accepted that this moisture source was controlled by uplift of the Tian Shan and Pamir orographic barriers established since the mid-Miocene (*18*, *108*, *129*). This explains why the Tarim Basin/southern Tian Shan (locality 1; Fig. 6) never displays a meaningful grass presence, whereas the Junggar Basin/northern Tian Shan (locality 2; Fig. 6) records grasses from 7 Ma (locality 3 is also in the northern Tian Shan but higher upslope; thus, it received mainly arboreal pollen and does not record a meaningful grass presence either; Fig. 6). However, there is no particular uplift expressed regionally in these mountain ranges that could explain the shift at 7 Ma, thus requiring alternative potential driving mechanisms.

C_3-C_4 photosynthetic pathways

Direct estimates of C_4 vegetation proportions in Miocene Central Asia with good age control remain lacking, but we hypothesize that the mid-Miocene radiation of herbs in eastern Central Asia could also have been partly enabled by the C_4 photosynthetic pathway. This evolutionary innovation improves water use efficiency under low levels of atmospheric pCO_2 in hot, open, and seasonally dry/saline environments, where photorespiration is particularly high in C_3 plant species (*105*, *130*, *131*). Specifically in the semiarid Central Asian region, C_4 vegetation appears to be favored by increased warm-season rainfall and higher temperatures (*111*, *132*). Humid conditions are documented in several records [e.g., (*18*, *79*, *92*, *98*, *99*, *103*, *107*, *133*, *134*)] during the MMCO (16.8 to 14.7 Ma; (*112*)], the timing of which coincides with the presence of C_4 vegetation extrapolated from soil and tooth enamel $\delta^{13}C$ records in northern China, associated with an intensified summer monsoon (*115*).

Together, these data suggest that wetter conditions in parts of Central Asia, combined with declining atmospheric pCO_2, may have assisted C_4 grasses and herbs such as the Chenopodioideae to spread across the landscape (Fig. 6) (*132*), marking the transition from phase 2 to phase 3 (Fig. 5). Increased moisture levels during the MMCO would have been sufficient to reestablish a sufficient vegetation biomass: islands of fertility that could endure late Miocene aridity by means of a positive feedback loop [discussed in the previous sections; (*70*, *71*)]. After the MMCO, conditions became more arid, seasonal, and atmospheric pCO_2 dwindled (Fig. 5), and a second expansion of grasses and other herbs at 7 Ma occurred in both western and eastern Central Asia (Figs. 5 and 6). This second expansion is consistent with the global spread of C_4 grasses starting in the late Miocene (*40*, *105*, *106*); however, the dominant plant/grass species in grasslands today are tightly clustered within particular clades. This implies that characteristics besides the C_4 pathway played a role in their rise to dominance, which remains an unanswered question (*40*, *131*).

MODERN ECOREGION ANALOGS

Changes in vegetation, faunal composition, and climate indicate three distinct phases in the Cenozoic evolution of the Central Asian steppe-desert biome (Fig. 5): (i) warm shrub steppe-desert from the

middle Eocene, (ii) temperate desert/forested uplands from the EOT to the mid-late Miocene, and (iii) cold-temperate herb steppe from the mid-late Miocene until the modern day. Statistical analyses (figs. S1 and S3) indicate that phases 1, 2, and 3 differ significantly from each other in terms of floral assemblages, with phase 1 being dominated by *Ephedra* and *Nitraria* and phase 2 by high amounts of *Pinus*. The vegetational assemblage of phase 3 overlaps with the Holocene and modern vegetation of the region, and both are defined by *Artemisia* (Asteraceae), Poaceae, Chenopodioideae, and Cyperaceae: These are the key taxa in the modern herb steppe (Fig. 1).

Vegetation cover in these three phases can each be linked to a modern ecoregion analog using normalized difference vegetation index (NDVI) models of extant Asian steppe-deserts (Fig. 5 and tables S3 and S4). Compared to today, vegetation cover during phase 1 of the desert-steppe biome was similar to modern wet deserts like the Gurbantunggut, which hosts a relatively high proportion of plant biomass for such a precipitation-limited environment (Fig. 5 and table S4). This is achieved through low-lying islands of fertility between the sand dunes that trap runoff water and nutrients from the surrounding unvegetated land, leading to pronounced self-organizing spatial patterns such as tiger bush [Fig. 5 (1)] (*63*, *70*, *72*). During phase 2, vegetation density in valley basins would have dropped to lower levels as in the modern Taklimakan Desert (table S4), with high areas of biomass only directly surrounding water bodies or along the flanks of the basin at higher elevations [Fig. 5 (2)]. Because of regional topographic growth, new elevation-dependent ecological zones were created during phase 3, and vegetation cover became more variable than the previous phases. This resembles the modern Jinghe mountain–desert ecotone (Fig. 5 (3) and table S4), which incorporates a number of vegetation belts that display a vertical gradient from full coverage (mountain grassland above the treeline) to no coverage (low-elevation deserts).

The above three successive phases, or "stable states," that existed in the Central Asian steppe-desert were separated by two regime shifts, one at the EOT and one in the mid-Miocene. Although the dynamics of these shifts differed, both caused large-scale and irreversible ecosystem changes in the arid lands of Central Asia. On the basis of these past transitions to a new stable state (with very different biotic structures and distributions to the previous state), our synthesis suggests it unlikely that the modern steppe-desert will recover its present environmental configuration if forced into a new ecosystem phase by current anthropogenically induced global changes.

Climate model predictions, experimental studies, and recent climate records (*135*–*140*) point toward Central Asia becoming one of the hottest and driest regions on the planet in the near future. Major predicted changes include (i) highly reduced vegetation cover and rapid, severe species losses; (ii) increased precipitation variability; and (iii) widespread desertification and erosion generating elevated dust emissions. This new hyperarid desert phase would resemble that of the Oligocene–early Miocene (phase 2), with negative implications for future Asian biodiversity and human well-being.

CONCLUSIONS AND FUTURE DIRECTIONS

Our review illustrates that in a chorological-climatic sense, the Central Asian steppe-desert originated at least in the early–middle Eocene, but ecologically and physiognomically, it has evolved significantly from its early existence until the present day. The comparison of Paleogene and Neogene datasets shows that the "modern" herb-dominated Central Asian steppes have a relatively recent geological origin that is closely related to both topographic growth in the Tibetan region and Mio–Pliocene cooling. The initial late Miocene spread of herbs was made possible by tectonic, atmospheric, and climatic changes that created favorable microhabitats for floral exploitation, possibly combined with the evolution of new environmental niche tolerances in some C_4 herbs. However, colder temperatures limit the abundance of C_4 species across the Eurasian steppes today, on a northwest to southeast temperature gradient associated with summer monsoon penetration (*104*, *111*, *133*), and this begs the question of precisely when C_3 grasses became dominant across the Central Asian steppes.

Our synthesis has enabled the development of three major insights that can guide future work on Cenozoic ecosystems in Central Asia:

1. A unique shrub biome emerged in the Eocene steppe-desert, dominated by relatively rare or poorly represented taxa today (*Ephedra* and *Nitraria*). These plant families thus have a rich history that would have remained unknown if not for the palynological record (molecular phylogenies do not reveal the extent of their previous diversity), but further work is needed to understand their collapse in the latest Eocene and why they never again became common across the steppe-desert.

2. The EOT appears to have been the major determiner of steppe evolution in interior Asia, but data gaps and palynological records preserving few lowland taxa (being dominated instead by upslope arboreal pollen) mean that the Oligocene steppe remains an enigma for the present. In turn, the origins and drivers of structure and regime shifts in the drylands of Central Asia are still poorly understood. Future research should target localities that can improve our understanding of ecosystems before and after the EOT—particularly with regard to precipitation changes, which could help to elucidate the shrub-to-herb turnover in the steppe-desert environment.

3. The ecological radiations of herbs, including grasses, appear to be correlated with periods of increased moisture in the steppe-desert, in conjunction with declining atmospheric pCO_2 concentrations. Although a grass expansion at ~7 Ma in Central Asia appears linked with the global expansion of C_4 grasses, it remains unknown whether these Central Asian grasses were C_4 vegetation. Current data suggest the intriguing possibility that ecological radiations of C_4 grasses could have occurred before that of C_3 grasses in Central Asia, which is a reverse of the global pattern.

Future work should focus on an integration of palynological records, which give us a consistent picture of ecosystems through time, with macrobotanical fossils, molecular phylogenies, and C_3/C_4 abundance data (via phytoliths, carbon isotopes, and *n*-alkanes) from Cenozoic successions that are well constrained in time. This will enable a detailed reconstruction of the biotic and abiotic forces that have shaped steppe-desert evolution in Central Asia. Improving our understanding of previous regime shifts in the steppe-desert also reveals the resilience of this unique ecosystem to different environmental perturbations, which is relevant for quantifying the vulnerability of modern drylands in the face of climate change and land degradation (*73*).

MATERIALS AND METHODS

Delineation of the study area

We follow classification and subdivision conventions outlined for the Palaearctic steppe biome by the recent syntheses of Wesche *et al.*

(*1*) and Hurka *et al.* (*2*) and illustrated in Figs. 1 and 2. The biome can be subdivided chronologically-climatically into various steppe regions across Eurasia, which are united in all comprising extratropical, highly seasonal environments too dry to sustain significant growth of closed tall woody vegetation. The coldest, driest, and most seasonally extreme of these regions is located within the Central Asian continental interior and forms the focus of our study, spanning Mongolia, northern and western China, and western and central Tibet. The climate here is classified as cold arid steppe [Köppen climate BSk; (*141*)] and characterized by low precipitation and extreme seasonality, with the elevated Tibetan region being colder and slightly wetter than the Mongolian, northern and western Chinese regions that together comprise the unique Central Asian steppe-desert biome (*1*).

This is distinct from the "Middle Asian steppe" to the west (comprising southern Central Siberia, Kazakhstan, and the Irano-Turanian region), which receives predominant winter precipitation in contrast to the Central Asian summer rainfall regions of Mongolia and Tibet (*1*). It also excludes humid-semihumid eastern and southeastern parts of the Tibetan Plateau to the east of the modern 500-mm isoline of annual precipitation (*11*) that $\delta^{18}O$ data show have received southerly, likely monsoonal moisture for the past 55 Ma (*142*). Today, these areas are vegetated by alpine meadow and forest, and palaeobotanical and palynological records show they have been dominated by broad-leaved and coniferous forest through the Cenozoic (*11*, *143*–*145*), placing them beyond the scope of this review.

In our concept of the Central Asian steppe-desert biome, we include all of the various ecological-physiognomic steppe subtypes across the Central Asian steppe region. These include meadow-steppe, forest-steppe, alpine-steppe, and typical steppe, grading into semidesert and desert-steppes in the drier parts of southern Mongolia and northwestern China. As steppe subtypes vary in the predominance of C_3 grasses today (and presumably also have in the past), we deem it important to consider various steppe subtypes in attempting to understand fluctuations of grasses and other herbs within the region over long time scales. Furthermore, these steppe subtypes were included because of the regional nature of the palynological record, which would have preserved taxa from different environmental settings in any case.

Sampled sections

In our study, we focus on an extended "best record" from the Xining Basin in NE Tibet (eastern Central Asia) to understand ecosystem changes at one locality over the EOT as well as millions of years prior [the "best sections method"; (*146*)]. This approach avoids problems with temporal precision, accuracy of correlations, and local environmental change between different localities, all of which can confound true perceptions of changing diversity and underlying drivers on geological time scales. Although the best sections method is potentially limited in its ability to reflect a regional or global pattern, we complemented high-resolution local pollen data and carbonate growth temperatures with a regional compilation of independent well-dated (by means of palaeomagnetic and/or radioisotopic ages) mammalian faunal and pollen records from a restricted longitudinal gradient in Central Asia (Fig. 3, Fig. 5 and fig. S1) to explore large-scale vegetation trends in the steppe-desert biome through the Cenozoic. This synthesis provides additional support that ecosystem changes observed in NE Tibet can be extrapolated to the greater Central Asian steppe-desert region, but future studies on other independently dated reference sections should be carried out to further corroborate these trends.

Pollen

We collected pollen samples on fieldwork in NE Tibet and northeast of the Qaidam Basin [Dahonggou section; (*68*)] in the summers of 2016–2018, which were prepared according to standard palynological preparation methods. These data were integrated with other selected pollen records chosen for their extended length and independent age control (by means of palaeomagnetic and/or radioisotopic ages), to generate a composite Central Asian palynological dataset spanning 43 Ma (Fig. 5B) using Tilia 2.0 software (*147*). To do this, we selected individual records (fig. S1) across a restricted longitudinal gradient and considered sites within their palaeogeographic (Fig. 2) and sedimentary palaeoenvironmental context, to more precisely identify forcing mechanisms of each ecological transition. Pollen taxa were assigned to ecological groups according to their growth habit, phylogenetic relationships, and/or environmental niche (table S1). Processing methods for each record were carefully compared and found to be equivalent, thus avoiding overrepresentation of any particular type in different records.

Constrained incremental sums of squares cluster analysis (CONISS) with stratigraphic constraints (*148*) was conducted on the palynological dataset (considering all individual taxa), using pollen percentage values with square root transformation (Edwards and Cavalli Sforza's chord distance) to provide reference for pollen zonation. Results of the ordination are included as a dendrogram in fig. S1. We also performed a principal components analysis (PCA) of the palynological records to identify any structure in the data (fig. S3). A Holocene palynological dataset of the Qaidam Basin (*149*) was added as a recent reference pollen dataset to compare with older floral assemblages. In total, 95 palynological taxa were included in the PCA, but only taxa reaching 5% or higher in at least one sample were plotted (see table S5) to increase visibility of the figure. Both analyses were carried out in R (*150*).

To further confirm that we identified real trends of steppe-desert evolution through the Cenozoic, records were also compared omitting certain ecological groups (fig. S1B): wind-blown bisaccates, localized aquatics and ferns, and unidentified taxa or those with multiple affinities. Consistency of the timing and nature of the shrub-to-herb turnover both with and without inclusion of the above groups further supports that the selected records reflect true changes in xerophytic shrubs, herbs, and grasses through time.

Phylogenetic analyses

We compiled and analyzed a mammalian fossil dataset from Central Asia, using all available publications of Central Asian mammalian fossils and from the Paleobiology Database (https://paleobiodb.org/#/), to estimate origination and extinction rates through time at genus level. Analyses were performed in PyRate (*151*) using a reversible-jump Markov chain Monte Carlo (RJMCMC) algorithm to estimate heterogeneity of origination and extinction rates through time. Analyses were run for 10,000,000 MCMC iterations and repeated over 10 replicated datasets, in which the ages of occurrences had been randomized within the respective stratigraphic ranges to account for dating uncertainty. Preservation rates were allowed to vary across geological epochs and across lineages using the time-variable Poisson process [TPP + Gamma model; (*151*)]. After removing the

first 120% of iterations as burn-in and combining the output of the 10 replicates, we computed marginal origination and extinction rates through time as estimated by the RJMCMC algorithm. Net diversification rates were calculated as origination-extinction rates through time.

Palaeogeographies

We derived projections (WGS84) of palaeogeographic reconstructions at 60, 40, and 20 Ma [(*152*); https://map.paleoenvironment.eu/] from geodynamic rotation parameters in Atlantic Hotspot reference frame (*153*) and modified them according to a compilation of references (*154*–*158*). GPlates, GMT (Generic Mapping Tools), and QGIS (Quantum geographic information system) software were used to generate bathymetry (*159*) and coastlines (*160*) and to modify topo90 topography according to a broad compilation of references as well as geological (https://map.paleoenvironment.eu/) and paleontological databases (www.paleobiodb.org/). These palaeogeographies formed the boundary conditions for climate simulations.

Climate models

We ran late Eocene and early Oligocene simulations using the Earth system model (ESM) IPSL-CM5A2. For a full description of boundary conditions and technical specificities of the model, see Tardif *et al.* (*46*). The ESM includes the LMDz5 atmospheric model, the ORCHIDEE land surface and vegetation model and the NEMO (Nucleus for European Modelling of the Ocean, www.nemo-ocean.eu/) ocean and sea ice model. Atmosphere and ocean are coupled through the OASIS model. ORCHIDEE ensures appropriate routing of all freshwater runoff to the ocean. There is no lake module in this version of the model. Vegetation is simulated through 11 plant functional types (PFT): 8 forest PFTs (2 tropical, 3 temperate, and 3 boreal), 1 bare soil PFT, and 2 grass PFTs (C_3 and C_4). In our simulations, the C_4 grass PFT is deactivated because expansion of C_4 plants occurred later than the Oligocene.

The simulations were first run in a fully coupled mode with idealized fixed vegetation bands for 3000 years until the temperature of deep ocean layers reached quasi-equilibrium. Results were averaged over the last 100 years of each simulation and fed to the dynamic vegetation model (200-year runs) to retrieve PFT proportions and updated climatological values, averaged over the last 50 years. This procedure enabled us to quantify changes in MAT, MAP, bare soil, and conifer proportions of the vegetation composition across the EOT. We compared these model outputs with multiple geological climate proxies for the Xining Basin (coordinates: 39°N to 41°N and 97°E to 101°E).

We used a recent middle-late Eocene paleogeography with atmospheric pCO_2 concentrations of 1120 ppm typical of middle Eocene values (*46*, *152*). There are no prescribed ice sheets in our late Eocene experiments. The early Oligocene boundary conditions differ from that of the late Eocene because of the development of the Antarctic Ice Sheet (*55*, *161*). To comprehensively model the climatic impacts of the Eocene–Oligocene glaciation, we prescribed a full ice sheet over Antarctica and lowered the mean sea level by 70 m in our early Oligocene simulations. In addition, atmospheric pCO_2 concentrations were reduced to 560 ppm (*56*). In particular, the lower sea level leads to the retreat of the proto-Paratethys Sea. Solar constant was reduced to 1360.19 W m^{-2} in both the late Eocene and early Oligocene simulations, and orbital parameters were fixed at present day values.

Modern ecoregion analogs

We used NDVI models of modern Asian deserts (Fig. 5D and tables S3 and S4) as analogs to illustrate the three Cenozoic phases of the Central Asian steppe-desert, each of which is characterized by broadly similar depositional environments and dominant plant taxa to its ancient counterpart. NDVI values were used to indicate plant health and phenology, spatial density distributions, and productivity and biomass of ecosystems by measuring differences between near-infrared (NIR; which vegetation strongly reflects) and red light (which vegetation absorbs). Using the formula $\mathrm{NDVI} = \frac{(\mathrm{NIR} - \mathrm{Red})}{(\mathrm{NIR} + \mathrm{Red})}$ generates a value between −1 and +1. Areas of barren rock, sand, or snow usually show very low NDVI values (0.1 or less). Sparse vegetation, e.g., shrubs/grasslands/senescing crops, result in moderate NDVI values (approximately 0.2 to 0.5). High NDVI values (approximately 0.6 to 0.9) correspond to dense vegetation such as that found in temperate and tropical forests or crops at their peak growth stage. We used the Operational Land Imager (OLI), a remote sensing instrument onboard Landsat 8, to image three types of desert over the plant growing season. Images were downloaded from the U.S. Geological Survey website (http://glovis.usgs.gov) and preprocessed (including atmospheric and radiation correction) using the ERDAS (Earth Resources Data Analysis System) 2013 software package, and band5 (NIR) and band4 (Red) reflectance data were used to calculate NDVI values.

SUPPLEMENTARY MATERIALS

Supplementary material for this article is available at http://advances.sciencemag.org/cgi/content/full/6/41/eabb8227/DC1

REFERENCES AND NOTES

1. K. Wesche, D. Ambarlı, J. Kamp, P. Török, J. Treiber, J. Dengler, The Palaearctic steppe biome: A new synthesis. *Biodivers. Conserv.* **25**, 2197–2231 (2016).
2. H. Hurka, N. Friesen, K.-G. Bernhardt, B. Neuffer, S. Smirnov, A. Shmakov, F. Blattner, The Eurasian steppe belt: Status quo, origin and evolutionary history. *Turczaninowia* **22**, 5–71 (2019).
3. V. Mosbrugger, A. Favre, A. N. Muellner-Riehl, M. Päckert, A. Mulch, in *Mountains, Climate and Biodiversity*, C. Hoorn, A. Perrigo, A. Antonelli, Eds. (John Wiley & Sons, 2018), pp. 429–448.
4. Angiosperm Phylogeny Group, M. W. Chase, M. J. M. Christenhusz, M. F. Fay, J. W. Byng, W. S. Judd, D. E. Soltis, D. J. Mabberley, A. N. Sennikov, P. S. Soltis, P. F. Stevens, An update of the Angiosperm Phylogeny Group classification for the orders and families of flowering plants: APG IV. *Bot. J. Linn. Soc.* **181**, 1–20 (2016).
5. C. Hoorn, J. Straathof, H. A. Abels, Y. Xu, T. Utescher, G. Dupont-Nivet, A late Eocene palynological record of climate change and Tibetan Plateau uplift (Xining Basin, China). *Palaeogeogr. Palaeoclimatol. Palaeoecol.* **344–345**, 16–38 (2012).
6. A. Koutsodendris, F. J. Allstädt, O. A. Kern, I. Kousis, F. Schwarz, M. Vannacci, A. Woutersen, E. Appel, M. A. Berke, X. Fang, O. Friedrich, C. Hoorn, U. Salzmann, J. Pross, Late Pliocene vegetation turnover on the NE Tibetan Plateau (Central Asia) triggered by early Northern Hemisphere glaciation. *Glob. Planet. Change* **180**, 117–125 (2019).
7. U. Herzschuh, Reliability of pollen ratios for environmental reconstructions on the Tibetan Plateau. *J. Biogeogr.* **34**, 1265–1273 (2007).
8. E. J. Milner-Gulland, E. Kreuzberg-Mukhina, B. Grebot, S. Ling, E. Bykova, I. Abdusalamov, A. Bekenov, U. Gärdenfors, C. Hilton-Taylor, V. Salnikov, L. Stogova, Application of IUCN red listing criteria at the regional and national levels: A case study from Central Asia. *Biodivers. Conserv.* **15**, 1873–1886 (2006).
9. D. Ge, Z. Wen, L. Xia, Z. Zhang, M. Erbajeva, C. Huang, Q. Yang, Evolutionary history of lagomorphs in response to global environmental change. *PLOS ONE* **8**, e59668 (2013).
10. R. A. Spicer, Tibet, the Himalaya, Asian monsoons and biodiversity – In what ways are they related? *Plant Divers.* **39**, 233–244 (2017).
11. X. Sun, P. Wang, How old is the Asian monsoon system?—Palaeobotanical records from China. *Palaeogeogr. Palaeoclimatol. Palaeoecol.* **222**, 181–222 (2005).
12. B. Song, R. A. Spicer, K. Zhang, J. Ji, A. Farnsworth, A. C. Hughes, Y. Yang, F. Han, Y. Xu, T. Spicer, T. Shen, D. J. Lunt, G. Shi, Qaidam Basin leaf fossils show northeastern Tibet was high, wet and cool in the early Oligocene. *Earth Planet. Sci. Lett.* **537**, 116175 (2020).
13. Y. Miao, F. Wu, M. Herrmann, X. Yan, Q. Meng, Late early Oligocene East Asian summer monsoon in the NE Tibetan Plateau: Evidence from a palynological record from the Lanzhou Basin, China. *J. Asian Earth Sci.* **75**, 46–57 (2013).

14. D.-N. Wang, X.-Y. Sun, Y.-N. Zhao, Z. He, *The Study on the Micropaleobotany from Cretaceous–Tertiary of the Oil Bearing Basins in Some Regions of Qinghai and Xinjiang* (China Environmental Science Press, 1990).
15. L. H. Zhou, S. Z. Sun, G. C. Chen, *Vegetation of Qinghai Province (1: 1,000,000)* (China Science and Technology Press, 1990).
16. G. Dupont-Nivet, W. Krijgsman, C. G. Langereis, H. A. Abels, S. Dai, X. Fang, Tibetan plateau aridification linked to global cooling at the Eocene–Oligocene transition. *Nature* **445**, 635–638 (2007).
17. G. Dupont-Nivet, C. Hoorn, M. Konert, Tibetan uplift prior to the Eocene-Oligocene climate transition: Evidence from pollen analysis of the Xining Basin. *Geology* **36**, 987–990 (2008).
18. Y. Miao, M. Herrmann, F. Wu, X. Yan, S. Yang, What controlled Mid–Late Miocene long-term aridification in Central Asia?—Global cooling or Tibetan Plateau uplift: A review. *Earth Sci. Rev.* **112**, 155–172 (2012).
19. R. E. Bosboom, H. A. Abels, C. Hoorn, B. C. J. van den Berg, Z. Guo, G. Dupont-Nivet, Aridification in continental Asia after the Middle Eocene Climatic Optimum (MECO). *Earth Planet. Sci. Lett.* **389**, 34–42 (2014).
20. J. K. Caves, D. Y. Moragne, D. E. Ibarra, B. U. Bayshashov, Y. Gao, M. M. Jones, A. Zhamangara, A. V. Arzhannikova, S. G. Arzhannikov, C. P. Chamberlain, The Neogene de-greening of Central Asia. *Geology* **44**, 887–890 (2016).
21. L. Bougeois, G. Dupont-Nivet, M. de Rafélis, J. C. Tindall, J.-N. Proust, G.-J. Reichart, L. J. de Nooijer, Z. Guo, C. Ormukov, Asian monsoons and aridification response to Paleogene sea retreat and Neogene westerly shielding indicated by seasonality in Paratethys oysters. *Earth Planet. Sci. Lett.* **485**, 99–110 (2018).
22. X. Li, R. Zhang, Z. Zhang, Q. Yan, What enhanced the aridity in Eocene Asian inland: Global cooling or early Tibetan Plateau uplift? *Palaeogeogr. Palaeoclimatol. Palaeoecol.* **510**, 6–14 (2018).
23. X. Wang, B. Carrapa, Y. Sun, D. L. Dettman, J. B. Chapman, J. K. C. Rugenstein, M. T. Clementz, P. G. DeCelles, M. Wang, J. Chen, J. Quade, F. Wang, Z. Li, I. Oimuhammadzoda, M. Gadoev, G. Lohmann, X. Zhang, F. Chen, The role of the westerlies and orography in Asian hydroclimate since the late Oligocene. *Geology* **48**, 728–732 (2020).
24. A. Licht, M. van Cappelle, H. A. Abels, J.-B. Ladant, J. Trabucho-Alexandre, C. France-Lanord, Y. Donnadieu, J. Vandenberghe, T. Rigaudier, C. Lécuyer, D. Terry Jr., R. Adriaens, A. Boura, Z. Guo, A. N. Soe, J. Quade, G. Dupont-Nivet, J.-J. Jaeger, Asian monsoons in a late Eocene greenhouse world. *Nature* **513**, 501–506 (2014).
25. J. X. Li, L. P. Yue, A. P. Roberts, A. M. Hirt, F. Pan, L. Guo, Y. Xu, R. G. Xi, L. Guo, X. K. Qiang, C. C. Gai, Z. X. Jiang, Z. M. Sun, Q. S. Liu, Global cooling and enhanced Eocene Asian mid-latitude interior aridity. *Nat. Commun.* **9**, 3026 (2018).
26. A. Rohrmann, P. Kapp, B. Carrapa, P. W. Reiners, J. Guynn, L. Ding, M. Heizler, Thermochronologic evidence for plateau formation in central Tibet by 45 Ma. *Geology* **40**, 187–190 (2012).
27. C. Wang, J. Dai, X. Zhao, Y. Li, S. A. Graham, D. He, B. Ran, J. Meng, Outward-growth of the Tibetan Plateau during the Cenozoic: A review. *Tectonophysics* **621**, 1–43 (2014).
28. S. Guillot, F. Goussin, L. Airaghi, A. Replumaz, J. de Sigoyer, C. Cordier, How and when did the Tibetan Plateau grow? *Russ. Geol. Geophys.* **60**, 957–977 (2019).
29. Z.-h. Wu, Z.-h. Wu, P.-s. Ye, D.-g. Hu, H. Peng, Late Cenozoic environmental evolution of the Qinghai-Tibet Plateau as indicated by the evolution of sporopollen assemblages. *Geol. China* **33**, 973–974 (2006).
30. Z. T. Guo, B. Sun, Z. S. Zhang, S. Z. Peng, G. Q. Xiao, J. Y. Ge, Q. Z. Hao, Y. S. Qiao, M. Y. Liang, J. F. Liu, Q. Z. Yin, J. J. Wei, A major reorganization of Asian climate by the early Miocene. *Clim. Past* **4**, 153–174 (2008).
31. Z. T. Guo, W. F. Ruddiman, Q. Z. Hao, H. B. Wu, Y. S. Qiao, R. X. Zhu, S. Z. Peng, J. J. Wei, B. Y. Yuan, T. S. Liu, Onset of Asian desertification by 22 Myr ago inferred from loess deposits in China. *Nature* **416**, 159–163 (2002).
32. L.-M. Lu, L.-F. Mao, T. Yang, J.-F. Ye, B. Liu, H.-L. Li, M. Sun, J. T. Miller, S. Mathews, H.-H. Hu, Y.-T. Niu, D.-X. Peng, Y.-H. Chen, S. A. Smith, M. Chen, K.-L. Xiang, C.-T. Le, V.-C. Dang, A.-M. Lu, P. S. Soltis, D. E. Soltis, J.-H. Li, Z.-D. Chen, Evolutionary history of the angiosperm flora of China. *Nature* **554**, 234–238 (2018).
33. P. Ma, C. Wang, J. Meng, C. Ma, X. Zhao, Y. Li, M. Wang, Late Oligocene-early Miocene evolution of the Lunpola Basin, central Tibetan Plateau, evidences from successive lacustrine records. *Gondw. Res.* **48**, 224–236 (2017).
34. S. S. Renner, Available data point to a 4-km-high Tibetan Plateau by 40 Ma, but 100 molecular-clock papers have linked supposed recent uplift to young node ages. *J. Biogeogr.* **43**, 1479–1487 (2016).
35. U. Linnemann, T. Su, L. Kunzmann, R. A. Spicer, W.-N. Ding, T. E. V. Spicer, J. Zieger, M. Hofmann, K. Moraweck, A. Gärtner, A. Gerdes, L. Marko, S.-T. Zhang, S.-F. Li, H. Tang, J. Huang, A. Mulch, V. Mosbrugger, Z.-K. Zhou, New U-Pb dates show a Paleogene origin for the modern Asian biodiversity hot spots. *Geology* **46**, 3–6 (2018).
36. J. Meng, M. C. McKenna, Faunal turnovers of Palaeogene mammals from the Mongolian Plateau. *Nature* **394**, 364–367 (1998).
37. B. P. Kraatz, J. H. Geisler, Eocene–Oligocene transition in Central Asia and its effects on mammalian evolution. *Geology* **38**, 111–114 (2010).
38. J. Sun, X. Ni, S. Bi, W. Wu, J. Ye, J. Meng, B. F. Windley, Synchronous turnover of flora, fauna and climate at the Eocene–Oligocene Boundary in Asia. *Sci. Rep.* **4**, 7463 (2014).
39. M. Page, A. Licht, G. Dupont-Nivet, N. Meijer, N. Barbolini, C. Hoorn, A. Schauer, K. Huntington, D. Bajnai, J. Fiebig, A. Mulch, Z. Guo, Synchronous cooling and decline in monsoonal rainfall in northeastern Tibet during the fall into the Oligocene icehouse. *Geology* **47**, 203–206 (2019).
40. C. A. E. Strömberg, Evolution of grasses and grassland ecosystems. *Annu. Rev. Earth Planet. Sci.* **39**, 517–544 (2011).
41. E. B. Leopold, L. Gengwu, C. Clay-Poole, in *Eocene-Oligocene Climatic and Biotic Evolution*, D. R. Prothero, W. A. Berggren, Eds. (Princeton Univ. Press, 1992), pp. 399–420.
42. X. Li, *Fossil Floras of China Through the Geological Ages* (Guangdong Science and Technology Press, Guangzhou, 1995).
43. M. Y. Kaya, G. Dupont-Nivet, J.-N. Proust, P. Roperch, L. Bougeois, N. Meijer, J. Frieling, C. Fioroni, S. Özkan Altıner, E. Vardar, N. Barbolini, M. Stoica, J. Aminov, M. Mamtimin, G. Zhaojie, Paleogene evolution and demise of the proto-Paratethys Sea in Central Asia (Tarim and Tajik basins): Role of intensified tectonic activity at ca. 41 Ma. *Basin Res.* **31**, 461–486 (2019).
44. M. E. Katz, K. G. Miller, J. D. Wright, B. S. Wade, J. V. Browning, B. S. Cramer, Y. Rosenthal, Stepwise transition from the Eocene greenhouse to the Oligocene icehouse. *Nat. Geosci.* **1**, 329–334 (2008).
45. K. G. Miller, J. D. Wright, M. E. Katz, B. S. Wade, J. V. Browning, B. S. Cramer, Y. Rosenthal, in *Late Eocene Earth Hothouse Icehouse Impacts*, C. Koeberl, A. Montanari, Eds. (Geological Society of America Special Paper, 2009), vol. 452, pp. 169–178.
46. D. Tardif, F. Fluteau, Y. Donnadieu, G. Le Hir, J.-B. Ladant, P. Sepulchre, A. Licht, F. Poblete, G. Dupont-Nivet, The origin of Asian monsoons: A modelling perspective. *Clim. Past* **16**, 847–865 (2020).
47. B.-Y. Geng, J.-R. Tao, G.-P. Xie, Early Tertiary fossil plants and paleoclimate of Lanzhou Basin. *Acta Phytotaxon. Sin.* **39**, 105–115 (2001).
48. F. Wu, D. Miao, M. Chang, G. Shi, N. Wang, Fossil climbing perch and associated plant megafossils indicate a warm and wet central Tibet during the late Oligocene. *Sci. Rep.* **7**, 878 (2017).
49. T. Su, A. Farnsworth, R. A. Spicer, J. Huang, F.-X. Wu, J. Liu, S.-F. Li, Y.-W. Xing, Y.-J. Huang, W.-Y.-D. Deng, H. Tang, C.-L. Xu, F. Zhao, G. Srivastava, P. J. Valdes, T. Deng, Z.-K. Zhou, No high Tibetan Plateau until the Neogene. *Sci. Adv.* **5**, eaav2189 (2019).
50. J. Liu, T. Su, R. A. Spicer, H. Tang, W.-Y.-D. Deng, F.-X. Wu, G. Srivastava, T. Spicer, T. Van Do, T. Deng, Z.-K. Zhou, Biotic interchange through lowlands of Tibetan Plateau suture zones during Paleogene. *Palaeogeogr. Palaeoclimatol. Palaeoecol.* **524**, 33–40 (2019).
51. S. L. Low, T. Su, T. E. V. Spicer, F.-X. Wu, T. Deng, Y.-W. Xing, Z.-K. Zhou, Oligocene *Limnobiophyllum* (Araceae) from the central Tibetan Plateau and its evolutionary and palaeoenvironmental implications. *J. Syst. Palaeontol.* **18**, 415–431 (2020).
52. R. A. Spicer, T. Su, P. J. Valdes, A. Farnsworth, F.-X. Wu, G. Shi, T. E. V. Spicer, Z. Zhou, Why 'the Uplift of the Tibetan Plateau' is a myth. *Natl. Sci. Rev.* , nwaa091 (2020).
53. T. J. Brodribb, J. Pittermann, D. A. Coomes, Elegance versus Speed: Examining the Competition between Conifer and Angiosperm Trees. *Int. J. Plant Sci.* **173**, 673–694 (2012).
54. T. J. Brodribb, S. A. M. McAdam, G. J. Jordan, S. C. V. Martins, Conifer species adapt to low-rainfall climates by following one of two divergent pathways. *Proc. Natl. Acad. Sci. U.S.A.* **111**, 14489–14493 (2014).
55. R. M. DeConto, D. Pollard, Rapid Cenozoic glaciation of Antarctica induced by declining atmospheric CO_2. *Nature* **421**, 245–249 (2003).
56. M. Pagani, M. Huber, Z. Liu, S. M. Bohaty, J. Henderiks, W. Sijp, S. Krishnan, R. M. DeConto, The role of carbon dioxide during the onset of Antarctic glaciation. *Science* **334**, 1261–1264 (2011).
57. J. W. Dalling, L. A. Cernusak, K. Winter, J. Aranda, M. Garcia, A. Virgo, A. W. Cheesman, A. Baresch, C. Jaramillo, B. L. Turner, Two tropical conifers show strong growth and water-use efficiency responses to altered CO_2 concentration. *Ann. Bot.* **118**, 1113–1125 (2016).
58. R. Zhang, V. A. Kravchinsky, L. Yue, Link between global cooling and mammalian transformation across the Eocene–Oligocene boundary in the continental interior of Asia. *Int. J. Earth Sci.* **101**, 2193–2200 (2012).
59. P. E. Tarasov, R. Cheddadi, J. Guiot, S. Bottema, O. Peyron, J. Belmonte, V. Ruiz-Sanchez, F. Saadi, S. Brewer, A method to determine warm and cool steppe biomes from pollen data; application to the Mediterranean and Kazakhstan regions. *J. Quat. Sci. Publ. Quat. Res. Assoc.* **13**, 335–344 (1998).
60. P. Cour, Z. Zheng, D. Duzer, M. Calleja, Z. Yao, Vegetational and climatic significance of modern pollen rain in northwestern Tibet. *Rev. Palaeobot. Palynol.* **104**, 183–204 (1999).

61. U. Herzschuh, K. Winter, B. Wünnemann, S. Li, A general cooling trend on the central Tibetan Plateau throughout the Holocene recorded by the Lake Zigetang pollen spectra. *Quat. Int.* **154–155**, 113–121 (2006).
62. Y. Pan, S. Yan, H. Behling, G. Mu, Transport of airborne *Picea schrenkiana* pollen on the northern slope of Tianshan Mountains (Xinjiang, China) and its implication for paleoenvironmental reconstruction. *Aerobiologia* **29**, 161–173 (2013).
63. M. Scheffer, S. R. Carpenter, Catastrophic regime shifts in ecosystems: Linking theory to observation. *Trends Ecol. Evol.* **18**, 648–656 (2003).
64. N. Meijer, G. Dupont-Nivet, H. A. Abels, M. Y. Kaya, A. Licht, M. Xiao, Y. Zhang, P. Roperch, M. Poujol, Z. Lai, Z. Guo, Central Asian moisture modulated by proto-Paratethys Sea incursions since the early Eocene. *Earth Planet. Sci. Lett.* **510**, 73–84 (2019).
65. P. Kapp, P. G. DeCelles, Mesozoic–Cenozoic geological evolution of the Himalayan-Tibetan orogen and working tectonic hypotheses. *Am. J. Sci.* **319**, 159–254 (2019).
66. B. Carrapa, P. G. DeCelles, X. Wang, M. T. Clementz, N. Mancin, M. Stoica, B. Kraatz, J. Meng, S. Abdulov, F. Chen, Tectono-climatic implications of Eocene Paratethys regression in the Tajik basin of central Asia. *Earth Planet. Sci. Lett.* **424**, 168–178 (2015).
67. L. M. Staisch, N. A. Niemi, M. K. Clark, H. Chang, Eocene to late Oligocene history of crustal shortening within the Hoh Xil Basin and implications for the uplift history of the northern Tibetan Plateau. *Tectonics* **35**, 862–895 (2016).
68. W. Wang, W. Zheng, P. Zhang, Q. Li, E. Kirby, D. Yuan, D. Zheng, C. Liu, Z. Wang, H. Zhang, J. Pang, Expansion of the Tibetan Plateau during the neogene. *Nat. Commun.* **8**, 15887 (2017).
69. T. Blayney, G. Dupont-Nivet, Y. Najman, J.-N. Proust, N. Meijer, P. Roperch, E. R. Sobel, I. Millar, Z. Guo, Tectonic evolution of the Pamir recorded in the Western Tarim Basin (China): Sedimentologic and magnetostratigraphic analyses of the Aertashi section. *Tectonics* **38**, 492–515 (2019).
70. W. H. Schlesinger, J. F. Reynolds, G. L. Cunningham, L. F. Huenneke, W. M. Jarrell, R. A. Virginia, W. G. Whitford, Biological feedbacks in global desertification. *Science* **247**, 1043–1048 (1990).
71. S. Kéfi, M. Holmgren, M. Scheffer, When can positive interactions cause alternative stable states in ecosystems? *Funct. Ecol.* **30**, 88–97 (2016).
72. M. Rietkerk, M. C. Boerlijst, F. van Langevelde, R. Hillerislambers, J. van de Koppel, L. Kumar, H. H. T. Prins, A. M. de Roos, Self-organization of vegetation in arid ecosystems. *Am. Nat.* **160**, 524–530 (2002).
73. M. Berdugo, M. Delgado-Baquerizo, S. Soliveres, R. Hernández-Clemente, Y. Zhao, J. J. Gaitán, N. Gross, H. Saiz, V. Maire, A. Lehman, M. C. Rillig, R. V. Solé, F. T. Maestre, Global ecosystem thresholds driven by aridity. *Science* **367**, 787–790 (2020).
74. R. Ochoa-Hueso, D. J. Eldridge, M. Delgado-Baquerizo, S. Soliveres, M. A. Bowker, N. Gross, Y. Le Bagousse-Pinguet, J. L. Quero, M. García-Gómez, E. Valencia, T. Arredondo, L. Beinticinco, D. Bran, A. Cea, D. Coaguila, A. J. Dougill, C. I. Espinosa, J. Gaitán, R. T. Guuroh, E. Guzman, J. R. Gutiérrez, R. M. Hernández, E. Huber-Sannwald, T. Jeffries, A. Linstädter, R. L. Mau, J. Monerris, A. Prina, E. Pucheta, I. Stavi, A. D. Thomas, E. Zaady, B. K. Singh, F. T. Maestre, Soil fungal abundance and plant functional traits drive fertile island formation in global drylands. *J. Ecol.* **106**, 242–253 (2018).
75. L. A. Alibekov, S. L. Alibekova, Factors and consequences of desertification processes in the mountains of Central Asia. *Oecologia Mont.* **16**, 25–30 (2012).
76. X. Wang, Y. Yang, Z. Dong, C. Zhang, Responses of dune activity and desertification in China to global warming in the twenty-first century. *Glob. Planet. Change* **67**, 167–185 (2009).
77. H. A. Abels, G. Dupont-Nivet, G. Xiao, R. Bosboom, W. Krijgsman, Step-wise change of Asian interior climate preceding the Eocene-Oligocene Transition (EOT). *Palaeogeogr. Palaeoclimatol. Palaeoecol.* **299**, 399–412 (2011).
78. J. Sun, B. F. Windley, Onset of aridification by 34 Ma across the Eocene-Oligocene transition in Central Asia. *Geology* **43**, 1015–1018 (2015).
79. Z. Tang, Z. Ding, P. D. White, X. Dong, J. Ji, H. Jiang, P. Luo, X. Wang, Late Cenozoic central Asian drying inferred from a palynological record from the northern Tian Shan. *Earth Planet. Sci. Lett.* **302**, 439–447 (2011).
80. J. J. Hooker, M. E. Collinson, N. P. Sille, Eocene–Oligocene mammalian faunal turnover in the Hampshire Basin, UK: Calibration to the global time scale and the major cooling event. *J. Geol. Soc.* **161**, 161–172 (2004).
81. E. Costa, M. Garcés, A. Sáez, L. Cabrera, M. López-Blanco, The age of the "Grande Coupure" mammal turnover: New constraints from the Eocene–Oligocene record of the Eastern Ebro Basin (NE Spain). *Palaeogeogr. Palaeoclimatol. Palaeoecol.* **301**, 97–107 (2011).
82. M. Fortelius, J. T. Eronen, F. Kaya, H. Tang, P. Raia, K. Puolamäki, Evolution of Neogene mammals in Eurasia: Environmental forcing and biotic interactions. *Annu. Rev. Earth Planet. Sci.* **42**, 579–604 (2014).
83. J.-J. Châteauneuf, Palynostratigraphie et paléoclimatologie de l'Eocène supérieur et de F Oligocène du Bassin de Paris (France). *Mém. Bur. Rech. Géologiques Miniéres Fr.* **116**, 1–377 (1980).
84. M. J. Pound, U. Salzmann, Heterogeneity in global vegetation and terrestrial climate change during the late Eocene to early Oligocene transition. *Sci. Rep.* **7**, 43386 (2017).
85. M. E. Collinson, J. J. Hooker, Paleogene vegetation of Eurasia: Framework for mammalian faunas. *Deinsea* **10**, 41–84 (2003).
86. O. T. Burney, D. F. Jacobs, Ungulate herbivory of regenerating conifers in relation to foliar nutrition and terpenoid production. *For. Ecol. Manag.* **262**, 1834–1845 (2011).
87. F. Bognounou, P. E. Hulme, L. Oksanen, O. Suominen, J. Olofsson, Role of climate and herbivory on native and alien conifer seedling recruitment at and above the Fennoscandian tree line. *J. Veg. Sci.* **29**, 573–584 (2018).
88. N. Lobo, Conifer seed predation by terrestrial small mammals: A review of the patterns, implications, and limitations of top-down and bottom-up interactions. *For. Ecol. Manag.* **328**, 45–54 (2014).
89. H. Gomes Rodrigues, L. Marivaux, M. Vianey-Liaud, Expansion of open landscapes in Northern China during the Oligocene induced by dramatic climate changes: Paleoecological evidence. *Palaeogeogr. Palaeoclimatol. Palaeoecol.* **358–360**, 62–71 (2012).
90. J. T. Eronen, P. D. Polly, M. Fred, J. Damuth, D. C. Frank, V. Mosbrugger, C. Scheidegger, N. C. Stenseth, M. Fortelius, Ecometrics: The traits that bind the past and present together. *Integr. Zool.* **5**, 88–101 (2010).
91. M. Fortelius, J. T. Eronen, L. Liu, D. Pushkina, A. Tesakov, I. Vislobokova, Z. Zhaoqun, Continental-scale hypsodonty patterns, climatic paleobiogeography, and dispersal of Eurasian Neogene large mammal herbivores. *Deinsea* **10**, 1–11 (2003).
92. L. Liu, J. T. Eronen, M. Fortelius, Significant mid-latitude aridity in the middle Miocene of East Asia. *Palaeogeogr. Palaeoclimatol. Palaeoecol.* **279**, 201–206 (2009).
93. Y. Zhang, J. Zhan, *Late Cretaceous and Early Tertiary Spores and Pollen from the Western Tarim Basin, S. Xinjiang, China* (Science Press, 1991).
94. F. Yang, W. Tang, J. Wei, Z. Fu, S. Liang, *Tertiary in Petroliferous Regions of China II, The Northwest Region of China* (Petroleum Industry Press, 1994).
95. Y. Ma, J. Li, X. Fan, Pollen-based vegetational and climatic records during 30.6 to 5.0 My from Linxia area, Gansu. *Chin. Sci. Bull.* **43**, 301–304 (1998).
96. E. A. Macaulay, E. R. Sobel, A. Mikolaichuk, M. Wack, S. A. Gilder, A. Mulch, A. B. Fortuna, S. Hynek, F. Apayarov, The sedimentary record of the Issyk Kul basin, Kyrgyzstan: Climatic and tectonic inferences. *Basin Res.* **28**, 57–80 (2016).
97. J. Sun, Q. Xu, B. Huang, Late Cenozoic magnetochronology and paleoenvironmental changes in the northern foreland basin of the Tian Shan Mountains. *J. Geophys. Res. Solid Earth* **112**, B04107 (2007).
98. Z. Hui, J. Li, C. Song, J. Chang, J. Zhang, J. Liu, S. Liu, T. Peng, Vegetation and climatic changes during the Middle Miocene in the Wushan Basin, northeastern Tibetan Plateau: Evidence from a high-resolution palynological record. *J. Asian Earth Sci.* **147**, 116–127 (2017).
99. Z. Hui, J. Zhang, Z. Ma, X. Li, T. Peng, J. Li, B. Wang, Global warming and rainfall: Lessons from an analysis of Mid-Miocene climate data. *Palaeogeogr. Palaeoclimatol. Palaeoecol.* **512**, 106–117 (2018).
100. J. Liu, J. J. Li, C. H. Song, H. Yu, T. J. Peng, Z. C. Hui, X. Y. Ye, Palynological evidence for late Miocene stepwise aridification on the northeastern Tibetan Plateau. *Clim. Past* **12**, 1473–1484 (2016).
101. Y. Ma, X. Fang, J. Li, F. Wu, J. Zhang, The vegetation and climate change during Neocene and Early Quaternary in Jiuxi Basin, China. *Sci. China Ser. D Earth Sci.* **48**, 676 (2005).
102. H. Jiang, Z. Ding, Spatial and temporal characteristics of Neogene palynoflora in China and its implication for the spread of steppe vegetation. *J. Arid Environ.* **73**, 765–772 (2009).
103. J. Sun, Z. Zhang, Palynological evidence for the mid-Miocene climatic optimum recorded in Cenozoic sediments of the Tian Shan Range, northwestern China. *Glob. Planet. Change* **64**, 53–68 (2008).
104. E. J. Edwards, C. P. Osborne, C. A. E. Strömberg, S. A. Smith; C4 Grasses Consortium, The origins of C_4 grasslands: Integrating evolutionary and ecosystem science. *Science* **328**, 587–591 (2010).
105. C. P. Osborne, L. Sack, Evolution of C_4 plants: A new hypothesis for an interaction of CO_2 and water relations mediated by plant hydraulics. *Philos. Trans. R. Soc. B Biol. Sci.* **367**, 583–600 (2012).
106. E. J. Edwards, C. J. Still, Climate, phylogeny and the ecological distribution of C4 grasses. *Ecol. Lett.* **11**, 266–276 (2008).
107. Y. Miao, X. Fang, M. Herrmann, F. Wu, Y. Zhang, D. Liu, Miocene pollen record of KC-1 core in the Qaidam Basin, NE Tibetan Plateau and implications for evolution of the East Asian monsoon. *Palaeogeogr. Palaeoclimatol. Palaeoecol.* **299**, 30–38 (2011).
108. Z. Zhang, J. Sun, Palynological evidence for Neogene environmental change in the foreland basin of the southern Tianshan range, northwestern China. *Glob. Planet. Change* **75**, 56–66 (2011).
109. M. Cai, X. Fang, F. Wu, Y. Miao, E. Appel, Pliocene–Pleistocene stepwise drying of Central Asia: Evidence from paleomagnetism and sporopollen record of the deep borehole SG-3 in the western Qaidam Basin, NE Tibetan Plateau. *Glob. Planet. Change* **94-95**, 72–81 (2012).

110. J. Li, X. Fang, C. Song, B. Pan, Y. Ma, M. Yan, Late Miocene–Quaternary rapid stepwise uplift of the NE Tibetan Plateau and its effects on climatic and environmental changes. *Quatern. Res.* **81**, 400–423 (2014).
111. Z. An, Y. Huang, W. Liu, Z. Guo, S. Clemens, L. Li, W. Prell, Y. Ning, Y. Cai, W. Zhou, B. Lin, Q. Zhang, Y. Cao, X. Qiang, H. Chang, Z. Wu, Multiple expansions of C4 plant biomass in East Asia since 7 Ma coupled with strengthened monsoon circulation. *Geology* **33**, 705–708 (2005).
112. A. Holbourn, W. Kuhnt, M. Lyle, L. Schneider, O. Romero, N. Andersen, Middle Miocene climate cooling linked to intensification of eastern equatorial Pacific upwelling. *Geology* **42**, 19–22 (2014).
113. M. Steinthorsdottir, P. E. Jardine, W. C. Rember, Near-future pCO_2 during the hot mid Miocene Climatic Optimum. *Paleoceanogr. Paleoclimatol.* , e2020PA003900 (2020).
114. M. Fortelius, Z. Zhang, An oasis in the desert? History of endemism and climate in the late Neogene of North China. *Palaeontographica. Abt. A: Palaeozoologie - Stratigraphie* **277**, 131–141 (2006).
115. B. H. Passey, L. K. Ayliffe, A. Kaakinen, Z. Zhang, J. T. Eronen, Y. Zhu, L. Zhou, T. E. Cerling, M. Fortelius, Strengthened East Asian summer monsoons during a period of high-latitude warmth? Isotopic evidence from Mio-Pliocene fossil mammals and soil carbonates from northern China. *Earth Planet. Sci. Lett.* **277**, 443–452 (2009).
116. J.-Q. Liu, Y.-W. Duan, G. Hao, X.-J. Ge, H. Sun, Evolutionary history and underlying adaptation of alpine plants on the Qinghai–Tibet Plateau. *J. Syst. Evol.* **52**, 241–249 (2014).
117. J. Wen, J.-Q. Zhang, Z.-L. Nie, Y. Zhong, H. Sun, Evolutionary diversifications of plants on the Qinghai-Tibetan Plateau. *Front. Genet.* **5**, 4 (2014).
118. O. Hagen, L. Vaterlaus, C. Albouy, A. Brown, F. Leugger, R. E. Onstein, C. N. de Santana, C. R. Scotese, L. Pellissier, Mountain building, climate cooling and the richness of cold-adapted plants in the Northern Hemisphere. *J. Biogeogr.* **46**, 1792–1807 (2019).
119. M.-L. Zhang, X.-G. Xiang, J.-J. Xue, S. C. Sanderson, P. W. Fritsch, Himalayan uplift shaped biomes in Miocene temperate Asia: Evidence from leguminous *Caragana*. *Sci. Rep.* **6**, 36528 (2016).
120. N. Azani, A. Bruneau, M. F. Wojciechowski, S. Zarre, Miocene climate change as a driving force for multiple origins of annual species in *Astragalus* (Fabaceae, Papilionoideae). *Mol. Phylogenet. Evol.* **137**, 210–221 (2019).
121. M. Lauterbach, M. C. Veranso-Libalah, A. P. Sukhorukov, G. Kadereit, Biogeography of the xerophytic genus *Anabasis* L. (Chenopodiaceae). *Ecol. Evol.* **9**, 3539–3552 (2019).
122. Y. Xu, K. Zhang, Y. Yang, G. Wang, M. Luo, J. Ji, B. Song, Neogene evolution of the north-eastern Tibetan Plateau based on sedimentary, paleoclimatic and tectonic evidence. *Palaeogeogr. Palaeoclimatol. Palaeoecol.* **512**, 33–45 (2018).
123. D.-Y. Yuan, W.-P. Ge, Z.-W. Chen, C.-Y. Li, Z.-C. Wang, H.-P. Zhang, P.-Z. Zhang, D.-W. Zheng, W.-J. Zheng, W. H. Craddock, K. E. Dayem, A. R. Duvall, B. G. Hough, R. O. Lease, J.-D. Champagnac, D. W. Burbank, M. K. Clark, K. A. Farley, C. N. Garzione, E. Kirby, P. Molnar, G. H. Roe, The growth of northeastern Tibet and its relevance to large-scale continental geodynamics: A review of recent studies. *Tectonics* **32**, 1358–1370 (2013).
124. J. K. Caves, M. J. Winnick, S. A. Graham, D. J. Sjostrom, A. Mulch, C. P. Chamberlain, Role of the westerlies in Central Asia climate over the Cenozoic. *Earth Planet. Sci. Lett.* **428**, 33–43 (2015).
125. L. Bougeois, M. de Rafélis, G.-J. Reichart, L. J. de Nooijer, G. Dupont-Nivet, Mg/Ca in fossil oyster shells as palaeotemperature proxy, an example from the Palaeogene of Central Asia. *Palaeogeogr. Palaeoclimatol. Palaeoecol.* **441**, 611–626 (2016).
126. L. Ding, R. A. Spicer, J. Yang, Q. Xu, F. Cai, S. Li, Q. Lai, H. Wang, T. E. V. Spicer, Y. Yue, A. Shukla, G. Srivastava, M. A. Khan, S. Bera, R. Mehrotra, Quantifying the rise of the Himalaya orogen and implications for the South Asian monsoon. *Geology* **45**, 215–218 (2017).
127. P. D. Clift, K. V. Hodges, D. Heslop, R. Hannigan, H. Van Long, G. Calves, Correlation of Himalayan exhumation rates and Asian monsoon intensity. *Nat. Geosci.* **1**, 875–880 (2008).
128. P. Molnar, W. R. Boos, D. S. Battisti, Orographic controls on climate and paleoclimate of Asia: Thermal and mechanical roles for the Tibetan Plateau. *Annu. Rev. Earth Planet. Sci.* **38**, 77–102 (2010).
129. J. Sun, Z. Zhang, L. Zhang, New evidence on the age of the Taklimakan Desert. *Geology* **37**, 159–162 (2009).
130. R. F. Sage, The evolution of C_4 photosynthesis. *New Phytol.* **161**, 341–370 (2004).
131. E. J. Edwards, S. A. Smith, Phylogenetic analyses reveal the shady history of C_4 grasses. *Proc. Natl. Acad. Sci. U.S.A.* **107**, 2532–2537 (2010).
132. J. Dong, Z. Liu, Z. An, W. Liu, W. Zhou, X. Qiang, F. Lu, Mid-Miocene C_4 expansion on the Chinese Loess Plateau under an enhanced Asian summer monsoon. *J. Asian Earth Sci.* **158**, 153–159 (2018).
133. Y. Zhang, D. Sun, Z. Li, F. Wang, X. Wang, B. Li, F. Guo, S. Wu, Cenozoic record of aeolian sediment accumulation and aridification from Lanzhou, China, driven by Tibetan Plateau uplift and global climate. *Glob. Planet. Change* **120**, 1–15 (2014).
134. J. Zan, X. Fang, M. Yan, W. Zhang, Y. Lu, Lithologic and rock magnetic evidence for the Mid-Miocene Climatic Optimum recorded in the sedimentary archive of the Xining Basin, NE Tibetan Plateau. *Palaeogeogr. Palaeoclimatol. Palaeoecol.* **431**, 6–14 (2015).
135. J. A. Klein, J. Harte, X.-Q. Zhao, Experimental warming causes large and rapid species loss, dampened by simulated grazing, on the Tibetan Plateau. *Ecol. Lett.* **7**, 1170–1179 (2004).
136. X. Gao, Y. Shi, D. Zhang, F. Giorgi, Climate change in China in the 21st century as simulated by a high resolution regional climate model. *Chin. Sci. Bull.* **57**, 1188–1195 (2012).
137. H. Chen, Projected change in extreme rainfall events in China by the end of the 21st century using CMIP5 models. *Chin. Sci. Bull.* **58**, 1462–1472 (2013).
138. B. Hewitson, A. C. Janetos, T. R. Carter, F. Giorgi, R. G. Jones, W.-T. Kwon, L. O. Mearns, E. L. F. Schipper, M. van Aalst, in *Climate Change 2014: Impacts, Adaptation, and Vulnerability: Part B: Regional Aspects: Contribution of Working Group II to the Fifth Assessment Report of the Intergovernmental Panel on Climate Change*, V. R. Barros, C. B. Field, D. J. Dokken, M. D. Mastrandrea, K. J. Mach, T. E. Bilir, M. Chatterjee, K. L. Ebi, Y. O. Estrada, R. C. Genova, B. Girma, E. S. Kissel, A. N. Levy, S. MacCracken, P. R. Mastrandrea, L. L. White, Eds. (Cambridge Univ. Press, 2014), pp. 1133–1197.
139. J. Huang, M. Ji, Y. Xie, S. Wang, Y. He, J. Ran, Global semi-arid climate change over last 60 years. *Climate Dynam.* **46**, 1131–1150 (2016).
140. T. Sternberg, M. Edwards, Desert Dust and Health: A Central Asian review and steppe case study. *Int. J. Environ. Res. Public Health* **14**, 1342 (2017).
141. M. Kottek, J. Grieser, C. Beck, B. Rudolf, F. Rubel, World Map of the Köppen-Geiger climate classification. *Meteorol. Z.* **15**, 259–263 (2006).
142. J. K. Caves Rugenstein, C. P. Chamberlain, The evolution of hydroclimate in Asia over the Cenozoic: A stable-isotope perspective. *Earth Sci. Rev.* **185**, 1129–1156 (2018).
143. J.-R. Tao, N.-Q. Du, Miocene flora from Markam County and fossil record of Betulaceae. *Acta Bot. Sin.* **29**, 649–655 (1987).
144. Q. Xu, X. Liu, L. Ding, Miocene high-elevation landscape of the eastern Tibetan Plateau. *Geochem. Geophys. Geosyst.* **17**, 4254–4267 (2016).
145. J. Wu, K. Zhang, Y. Xu, G. Wang, C. N. Garzione, J. Eiler, P. H. Leloup, P. Sorrel, G. Mahéo, Paleoelevations in the Jianchuan Basin of the southeastern Tibetan Plateau based on stable isotope and pollen grain analyses. *Palaeogeogr. Palaeoclimatol. Palaeoecol.* **510**, 93–108 (2018).
146. S. G. Lucas, Permian tetrapod extinction events. *Earth Sci. Rev.* **170**, 31–60 (2017).
147. E. C. Grimm, *TILIA v2.0.b.4 and TGView v2.0* (Illinois State Museum, 1991).
148. E. C. Grimm, CONISS: A FORTRAN 77 program for stratigraphically constrained cluster analysis by the method of incremental sum of squares. *Comput. Geosci.* **13**, 13–35 (1987).
149. Y. Zhao, Z. Yu, F. Chen, E. Ito, C. Zhao, Holocene vegetation and climate history at Hurleg Lake in the Qaidam Basin, northwest China. *Rev. Palaeobot. Palynol.* **145**, 275–288 (2007).
150. R. C. Team, *R: A language and environment for statistical computing* (R Foundation for Statistical Computing, 2013); www.R-project.org/.
151. D. Silvestro, N. Salamin, A. Antonelli, X. Meyer, Improved estimation of macroevolutionary rates from fossil data using a Bayesian framework. *Paleobiology* **45**, 546–570 (2019).
152. F. Poblete, G. Dupont-Nivet, A. Licht, D. J. J. van Hinsbergen, P. Roperch, F. Guillocheau, G. Baby, M. Baatsen, paper presented at the European Geosciences Union General Assembly, Vienna, Austria, 23 to 28 April 2017.
153. M. Seton, R.D. Müller, S. Zahirovic, C. Gaina, T. Torsvik, G. Shephard, A. Talsma, M. Gurnis, M. Turner, S. Maus, M. Chandler, Global continental and ocean basin reconstructions since 200 Ma. *Earth-Science Reviews* 113, 212–270 (2012).
154. D. J. J. van Hinsbergen, S. M. Schmid, Map view restoration of Aegean–West Anatolian accretion and extension since the Eocene. *Tectonics* **31**, TC5005 (2012).
155. N. McQuarrie, D. J. J. van Hinsbergen, Retrodeforming the Arabia-Eurasia collision zone: Age of collision versus magnitude of continental subduction. *Geology* **41**, 315–318 (2013).
156. D. J. J. van Hinsbergen, P. Kapp, G. Dupont-Nivet, P. C. Lippert, P. G. DeCelles, T. H. Torsvik, Restoration of Cenozoic deformation in Asia and the size of Greater India. *Tectonics* **30**, TC5003 (2011).
157. D. J. J. van Hinsbergen, P. C. Lippert, S. Li, W. Huang, E. L. Advokaat, W. Spakman, Reconstructing Greater India: Paleogeographic, kinematic, and geodynamic perspectives. *Tectonophysics* **760**, 69–94 (2019).
158. P. C. Lippert, D. J. J. van Hinsbergen, G. Dupont-Nivet, in *Toward an Improved Understanding of Uplift Mechanisms and the Elevation History of the Tibetan Plateau*, J. Nie, B. K. Horton, G. D. Hoke, Eds. (Geological Society of America Special Paper, 2014), vol. 507, pp. 1–21.
159. R. D. Müller, M. Sdrolias, C. Gaina, W. R. Roest, Age, spreading rates, and spreading asymmetry of the world's ocean crust. *Geochem. Geophys. Geosyst.* **9**, Q04006 (2008).
160. C. Heine, L. G. Yeo, R. D. Müller, Evaluating global paleoshoreline models for the Cretaceous and Cenozoic. *Aust. J. Earth Sci.* **62**, 275–287 (2015).

161. J.-B. Ladant, Y. Donnadieu, V. Lefebvre, C. Dumas, The respective role of atmospheric carbon dioxide and orbital parameters on ice sheet evolution at the Eocene-Oligocene transition. *Paleoceanography* **29**, 810–823 (2014).
162. L. Li, M. Fan, N. Davila, G. Jesmok, B. Mitsunaga, A. Tripati, D. Orme, Carbonate stable and clumped isotopic evidence for late Eocene moderate to high elevation of the east-central Tibetan Plateau and its geodynamic implications. *GSA Bull.* **131**, 831–844 (2019).
163. M. Steinthorsdottir, A. S. Porter, A. Holohan, L. Kunzmann, M. Collinson, J. C. McElwain, Fossil plant stomata indicate decreasing atmospheric CO_2 prior to the Eocene–Oligocene boundary. *Clim. Past* **12**, 439–454 (2016).
164. G. L. Foster, D. L. Royer, D. J. Lunt, Future climate forcing potentially without precedent in the last 420 million years. *Nat. Commun.* **8**, 14845 (2017).
165. J. G. Ogg, G. M. Ogg, F. M. Gradstein, A Concise Geologic Time Scale: 2016 (Elsevier, 2016). 240 pp. 166.
166. B. S. Cramer, J. R. Toggweiler, J. D. Wright, M. E. Katz, K. G. Miller, Ocean overturning since the Late Cretaceous: Inferences from a new benthic foraminiferal isotope compilation. *Paleoceanography* **24**, PA4216 (2009).

Acknowledgments: We thank J. Sun, Y. Miao, and Y. Zhao for supplying original pollen counts; A. Milne for critical reading of the manuscript draft; and C. Jaramillo and R.A. Spicer for insightful reviews of the submitted paper. **Funding:** N.B., A.W., G.D.-N., D.T., N.M., and A.R. acknowledge funding from European Research Council consolidator grant MAGIC 649081. C.H. was supported by CAS President's International Fellowship Initiative Grant No. 2018VBA0038. D.S. received funding from the Swiss National Science Foundation (PCEFP3_187012; FN-1749). Climate modeling used the HPC resources of TGCC under the allocation 2018-A0050107601 made by GENCI. D.T., F.F., G.L.H., and Y.D. acknowledge funding from INSU-CNRS SYSTER. **Author contributions:** N.B., A.W., and C.H. conceived the initial study, identified and counted pollen, compiled the pollen datasets, designed figures, and performed analyses. G.D.-N. and D.S. provided conceptual input, designed figures, and performed analyses. N.B., A.W., G.D.-N., N.M., A.R., X.-J.L., Y.Z., C.H., and A.L. conducted fieldwork. G.D.-N. and D.T. produced the palaeogeographies. D.T., Y.D., F.F., J.-B.L., and G.L.H. performed the climate modeling experiments. P.M.C.C. compiled the mammalian data. C.C. and H.-X.Z. contributed NDVI models and images. A.L. provided clumped isotope data. A.K. and F.H. contributed pollen counts. C.R. reviewed molecular records. N.B. wrote the first draft, and all authors participated in the interpretation of the results and approved the final draft. **Competing interests:** The authors declare that they have no competing interests. **Data and materials availability:** All data needed to evaluate the conclusions in the paper are present in the paper and/or the Supplementary Materials. Correspondence and requests for materials should be addressed to N.B., A.W., or C.H. Additional data are available in the following repositories: https://figshare.com/articles/Pollen_data_JGR_2007_xls/12108507 and https://figshare.com/articles/Pollen_data_of_Zhang_Sunl_2011_GPC/12101442.

Submitted 20 March 2020
Accepted 20 August 2020
Published 9 October 2020
10.1126/sciadv.abb8227

Citation: N. Barbolini, A. Woutersen, G. Dupont-Nivet, D. Silvestro, D. Tardif, P. M. C. Coster, N. Meijer, C. Chang, H.-X. Zhang, A. Licht, C. Rydin, A. Koutsodendris, F. Han, A. Rohrmann, X.-J. Liu, Y. Zhang, Y. Donnadieu, F. Fluteau, J.-B. Ladant, G. Le Hir, C. Hoorn, Cenozoic evolution of the steppe-desert biome in Central Asia. *Sci. Adv.* **6**, eabb8227 (2020).

Science Advances

Cenozoic evolution of the steppe-desert biome in Central Asia

N. Barbolini, A. Woutersen, G. Dupont-Nivet, D. Silvestro, D. Tardif, P. M. C. Coster, N. Meijer, C. Chang, H.-X. Zhang, A. Licht, C. Rydin, A. Koutsodendris, F. Han, A. Rohrmann, X.-J. Liu, Y. Zhang, Y. Donnadieu, F. Fluteau, J.-B. Ladant, G. Le Hir and C. Hoorn

Sci Adv **6** (41), eabb8227.
DOI: 10.1126/sciadv.abb8227